Bulletin of the Earthquake
Research Institute
Vol. 45 (1967), pp. 417-471

24. Ground Cracks at Matsushiro Probably of Underlying Strike-slip Fault Origin, II —The Matsushiro Earthquake Fault.

By Kazuaki Nakamura and Yukimasa Tsuneishi,

Earthquake Research Institute.

(Read July 19, Sept. 27, 1966 and March 28, 1967.—Received March 31, 1967.)

Contents

1. Introduction

The Matsushiro earthquakes which started in early August, 1965, culminated in April, 1966, the maximum number and magnitude being over 600 felt shocks per day and 5.0 on the Richter scale[1]. During this

1) The Party for Seismographic Observation of Matsushiro Earthquakes and the Seismometrical Section, "Matsushiro Earthquakes Observed with a Temporary Seismographic Network, Parts 1, 2 and 3", *Bull. Earthq. Res. Inst.*, **44** (1966) 309, 702 and **45** (1967) 210.
Japan Meteorological Agency, "Preliminary report of Matsushiro swarm earthquakes" (in Japanese) Nos. 1, 2 and 3.

period, four linear ground fissure zones were successively formed in the middle of the epicentral area of the earthquakes which were a few hundred metres in length and arranged *en echelon*. Each linear zone consists of numerous open ground cracks a few to several metres in length. The component cracks in the zone are arranged uniformly *en echelon* indicating left-lateral movement. As gradual opening of the cracks were observed, the writers immediately started continuous measurement of displacement at six stations in the fissure zones.

Field observations and results of the crack measurement until early June, 1966, were reported in the first paper[2] and the hypothesis was tentatively offered that these cracks could be best explained by movement on a buried left-lateral strike-slip fault.

Following a period of lower seismicity in June and July, there came another peak to the earthquake swarm, August to September, 1966, the maximum magnitude and number being 5.0 and over 500 felt shocks per day. During this peak period, the four zones began to move again in the same sense as previously and, moreover, new fissure zones of similar nature appeared within and on the extension of the fissured area already defined by the earlier four zones. Movement during this period included not only horizontal but also systematic vertical displacement across fissure zones.

Seismic activity rapidly decreased again since the beginning of September. However, an unusual outflow of ground water and associated ground cracks, some of which developed into catastrophic landslides[3], occurred in the same general area as the fissured area defined by this study. These phenomena culminated at the end of September. As a consequence, problems arose on the distinction between ground cracks related to incipient landslides and those of tectonic origin. Water in the new springs contains a considerable amount of chloride and some springs are oversaturated with carbon dioxide*. Most of the oversaturated springs emerged through the ground cracks which are believed to be related to faulting.

Through this chain of events, the presence of a buried strike-slip

2) K. NAKAMURA and Y. TSUNEISHI, "Ground Cracks at Matsushiro probably of Underlying Strike-slip Fault Origin, I", *Bull. Earthq. Res. Inst.*, **44** (1966) 1371.

3) R. MORIMOTO, K. NAKAMURA, Y. TSUNEISHI, J. OSSAKA and N. TSUNODA, "The Landslides in the Epicentral Area of Matsushiro Earthquake Swarm—Their Relation to the Earthquake fault." ibid., **45** (1967) 241.

* Chemical aspects of these problems will be reported later by members of the Earthq. Res. Inst.

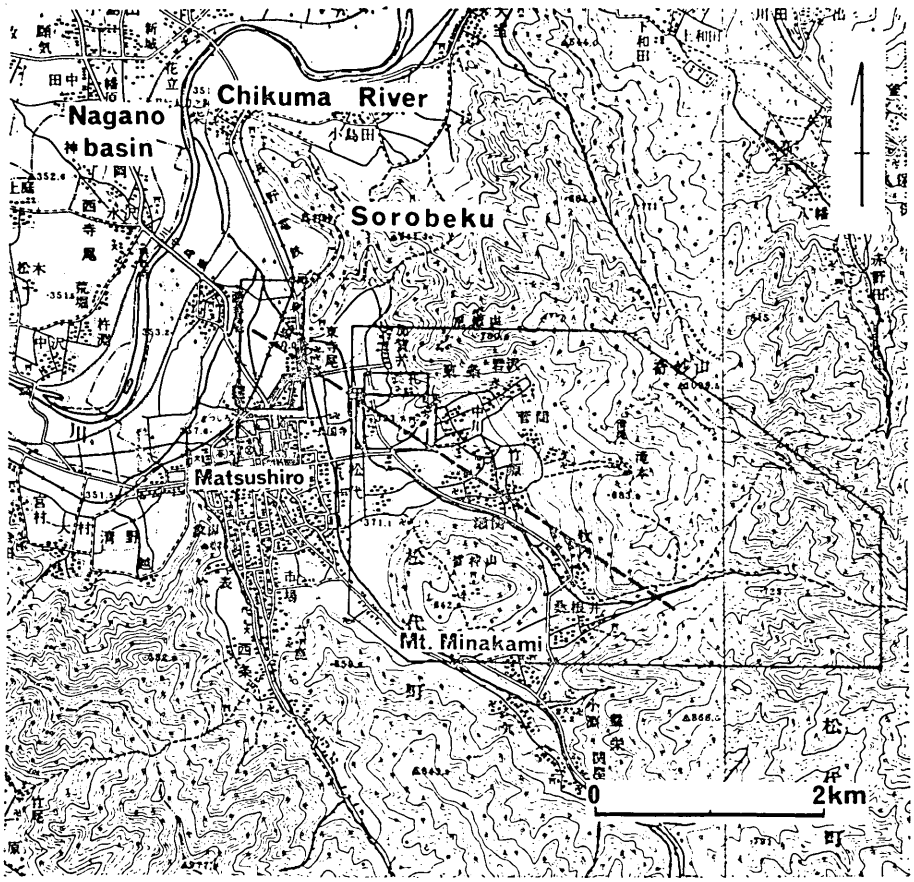

Fig. 10. Locality map. Location of Figs. 11, 44, 45a and 47 and the left-lateral fault or axis of the zone of strong deformation are shown.

earthquake fault or faults proposed in the first paper for the interpretation of some of the ground cracks, seems to have now become an almost undeniable fact. This paper describes 1) distribution of all of the ground cracks, 2) their genetic distinction and 3) the methods used and results of continuous displacement measurements across ground cracks and fissure zones. The inferred location and estimates of the amount of the displacement on the assumed left-lateral fault are also presented.

2. Description of fissure zones*

Classification of fissure zones

Distribution of fissure zones or groups of ground cracks as mapped by the writers up to march 1967 is shown in Fig. 11. Their distribution as of June, 1966 has already been shown in Figs. 1 and 2 of the first paper. Additional ground cracking was not observed until the end of August, 1966. From the end of August to October, 1966, or during and after the last culmination of seismicity, a number of ground cracks were formed some of which were associated with areal new ground water outflow. Since October no new cracks have developed and the older cracks have become more and more obscure in part as a result of winter frost and snow. By the spring of 1967 most of the cracks could be located in the field only indirectly by displaced structures such as the concrete base of a house. Volume of outflowing water has also decreased, leaving chemical precipitates at some of the springs.

The new ground cracks (August to October, 1966) are not only fissure

Table 2. Difference in the surface expression of nature of fissure zones (group of ground cracks) ascribed to movement of a buried strike-slip fault (*A*) and to landslides (slumping) in a broad sense (*B*).

	Echelon arrangement of component cracks within zone	Spatial distribution of zone	Relation to topography	
			Genenal trend of zone	Down-thrown side of zone
A	Uniform throughout	Limited to a narrow area trending in a NW direction, irrespective of geologic setting	Linear or slightly curved and not at all related	NE side (those with left-lateral displacement) SE side (those with right-lateral displacement)
B_1	Not uniform throughout. Often with reversed orientation at the ends	At the break in slope between highlands and flat alluvial lowlands	Generally parallel to contour lines	Downhill side
B_2		On the lower slopes of the highlands	Crescent shaped with concave side on the down-slope	

* A *fissure zone* is defined here as a group of open ground cracks which are naturally regarded to be of common origin by field observation. Therefore, fissure zones as thus defined include those of various origin. The *fissured area* is used in this paper as the area of distribution of left-lateral fissure zones of A-type (Table 2).

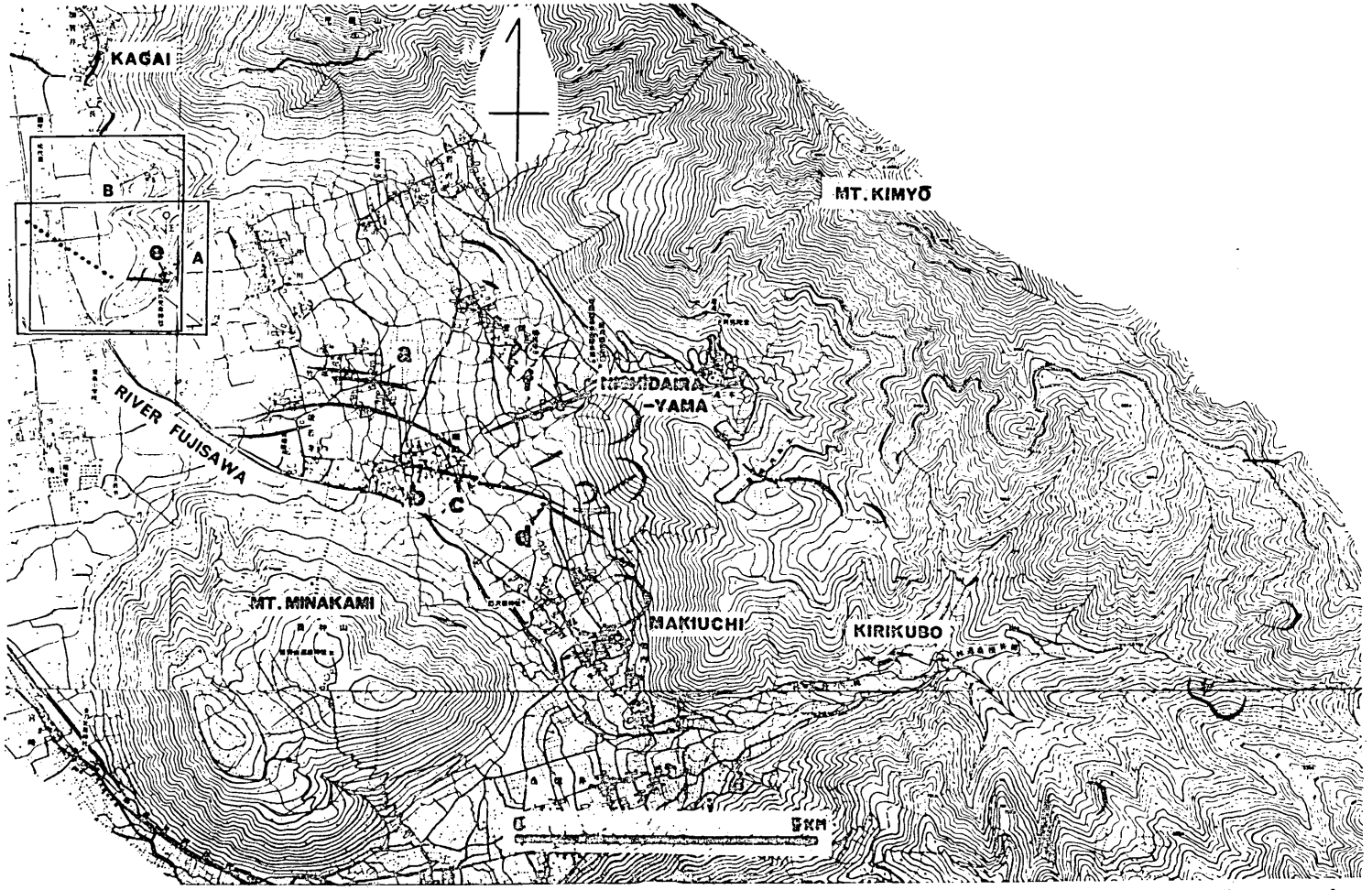

Fig. 11. Map showing the distribution of fissure zones (a group of ground cracks) regardless of their origin. There may be some more which the writers have not observed. Dotted line in the extreme left indicates the axis of deformation of concrete levees. Landslides are shown by thin dotted lines with fissure zones at Nishidaira-yama, Makiuchi, Kirikubo and the one in the lower right. Quadangles in the upper left are areas covered by Figs. 44(A) and 47(B).

zones of probable fault origin (A-type in Table 2) but include a number of zones which are attributable to landslides (B-type in Table 2). Field appearance of individual zones is superficially quite similar in some respects regardless of their origin, especially in that they all are comprised of short open ground cracks. But detailed observation made it nearly always possible to ascribe fissure zones to one of these two by using the various criteria summarized in Table 2.

It is most likely that fissure zones of B-type in the table formed by local down slope movements associated with rotational slump landslides or other forms of gravitational movements. The zones of B_1-type are those found at Kagai, Zozan, Nuruyu and other places. They are scattered widely throughout the epicentral area and are not restricted to the fissured area defined by the older four zones $F_1 \sim F_4$. Some of these zones appeared in 1965 during the initial phase of the earthquake swarm. Movement on them seems to be mainly related to the ground vibration by earthquakes attaining maximum rates during the culminate periods of seismicity.

The characteristic place of the formation of the B_1-type zone is on the talus-covered slopes where the mountains join flat alluvial plains. Small villages are often situated in such a place. In some of them houses that straddled the landslide block were severely damaged by slow rotational slumping of the lower side of the fissure zone. At the toe of the landslide block was observed also damage due to compression.

Those classified as B_2-type in the table appeared only during the period from middle September to early October, 1966. Occurrence of this type of zone is limited to the area northeast of Mt. Minakami on the lower slopes of mountains covered with thin talus debris. This area is the centre of both the epicentral area and intense vertial deformation of the ground associated with the earthquakes. It also coincides with the area of anomalous ground water outflow which started in late August, 1966. The zones of B_2-type at Nishidaira-yama, Makiuchi, Kirikubo and others developed into actual landslides a few to several days after their formation[4]. Movement of B_2-type fissure zones occurred at different times in different zones. Termination of the movement during middle October seems to have coincided with a marked decrease in the amount of ground water outflow from new springs.

General features of A-type fissure zones

Fissure zones of A-type are those ascribed to lateral movement of a

4) R. MORIMOTO et al., *loc. cit.*, 3).

Table 3. Data on fissure zones of *A*-type

Sign of fissure zones	Date of find (1966)	Length (m)		Trend	Maximum amount (cm) and sense of lateral displacement	Down-thrown side and maximum amount (cm)	Trend of component open cracks	Related Fig. No.
		(June)	(Sept.)					
F_1	(Jan. 21) April 11	275	290	80°W	Left 30	N 30	60°~75° E	4a,6,13,27
F_2	April 17	190	320	80°W	Left 10+	N 10	75°±10° E	
F_3	April 17	100	230	60°W	Left 20+	N 10	75° E	4b,14,28
F_4	May 18	130(+)	140(+)	80°−90°W	Left 10+	N? ?	45°~75° E	29
F_5	Aug. 20 (Sept. 4)	0	700(+)	65°W(−80° E)	Left 15+ (-neutral)	N 20	75°±10° E	
F_6	Aug. 28		370(+)	70° E	Right 10+	S 10	85°~80°W	31
F_7	end of Aug.		280	70°W(−90°W)	Left 15+	N 10	EW± 5°	
F_8	end of Aug.		230	80°W	Left 30	N 30	70°±10° E	15
F_9	end of Aug.		120(+)	75°−80°W	Left 2+	? 0?	75°	
F_{10}	end of Aug.		90(+)	55°W	Left 5+	N 5	75°±10°W	
F_{11}	end of Aug.		70(+)	85°W	Left 5+	N 10	75° E	
F_{12}	early Sept.		70(+)	65°−70°W	Left 5+	(N +)	80°± 5° E	
F_{13}	Sept. 11		240(+)	75°−90° E	(neutral?)	? 0?	?	
F_{14}	early Sept.(?)		100(+)	?	? 0	N 30	85°~90° E	16
F_{15}	Sept. 26		110(+)	65° E	Right 1+	?	80°W	
F_{16}	Feb. 20, 1967		190(+)	55° E	Right 10+	S 10	85°± 5° E	

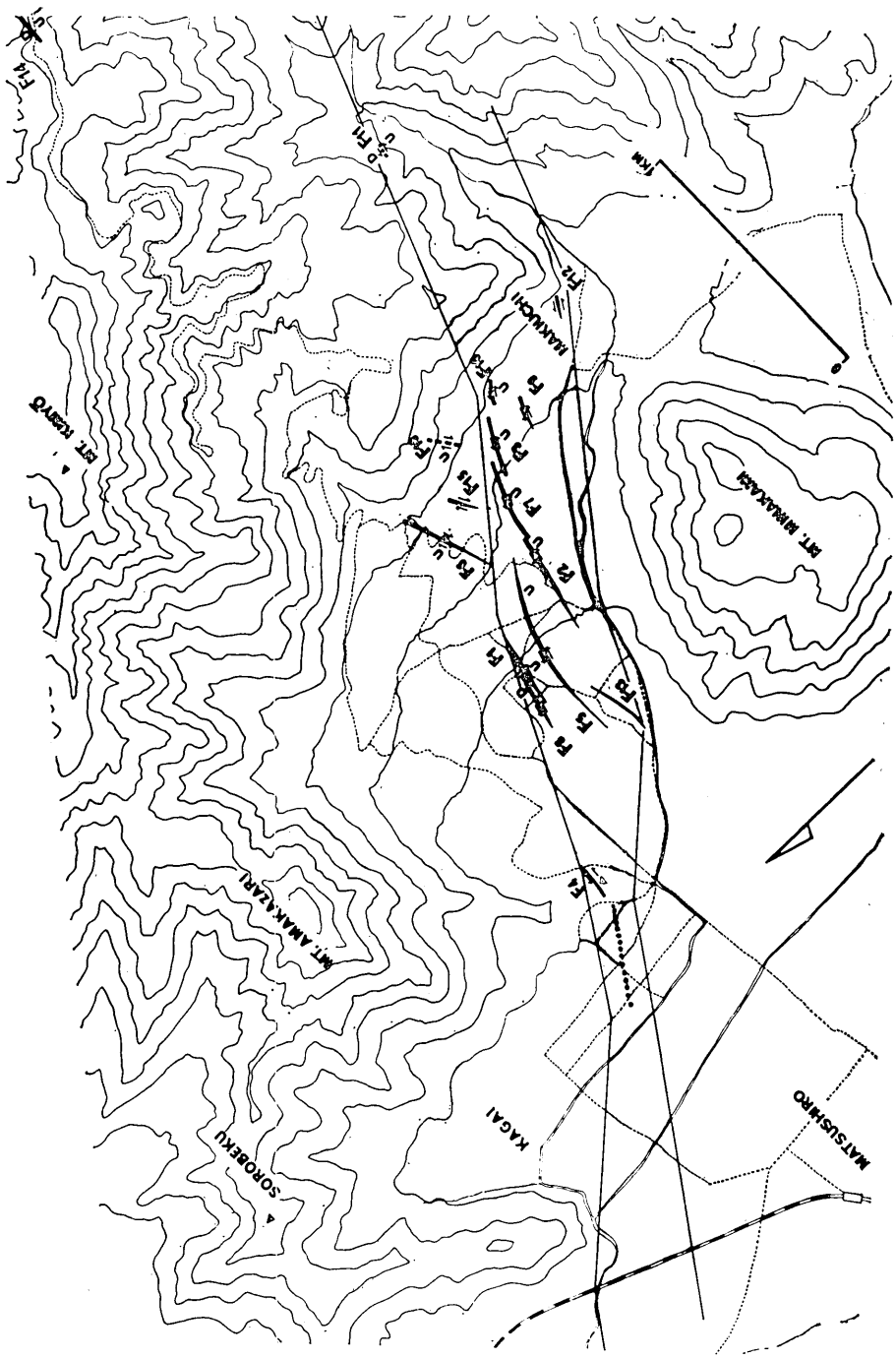

Fig. 12. Distribution of the fissure zones of probable fault origin or those which are unable to be attributed to landslide or the simple effect of gravity. The belt defined by two thin lines shows probable location of left-lateral buried fault. Broken lines indicate zones of doubtful origin. Two types of termination of fissure zones are distinguished; one is gradual dying out and the other is abrupt termination.

bedrock fault. These consist of short, parallel open cracks arranged *uniformly en echelon*. The width and displacement attain maxima in the middle part of the individual zones. Information on individual A-type fissure zones, such as date of find, length and trend of the zones, the trend of their component cracks, the sense of lateral movement indicated by crack orientation and the maximum amount of vertical and horizontal displacement on the fissure zones are summarized in Table 3. Distribution of the fissure zones is shown in Fig. 12.

The older four zones, $F_1 \sim F_4$, extended and showed additional left-lateral movement in August and September (Figs. 13 and 14). Two sets of fissure zones with differing lateral sense of movement are recognized among the new zones but the trends of component cracks in all the zones are similar in a general N80°E direction. Seven new zones trending N55°~85°W (F_5, $F_7 \sim F_{12}$), showed left-lateral movement distributed within, or on the extension of, the narrow fissured area defined by the older zones. Three new right-lateral zones of movement were also formed

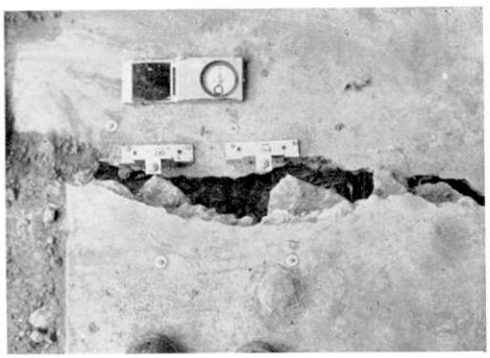

Fig. 13. Broken concrete slab at locality F_1-**a**, showing left-lateral displacement of crack A on Sept. 16, 1966. The same crack in April, May and June, 1966 was shown in Fig. 6 in the first paper. Oblique view is given in Fig. 27. Width of clinocompass is 6.5 cm.

Fig. 14. Left-lateral displacement about 20 cm along a crack in F_3. Although it is not clear from the photograph, this side of the crack is up-thrown by about 5 cm and separated by about 10 cm in the direction of the wall. The stone wall is mapped in Fig. 28. Scale 30 cm. Photograph taken March 9, 1967.

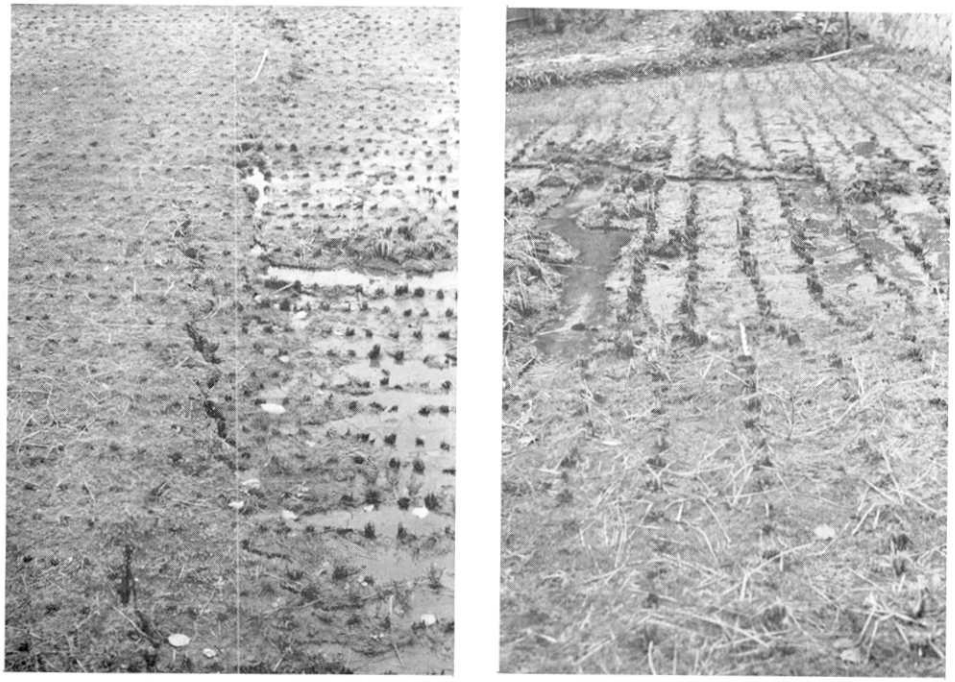

(a) (b)

Fig. 15. Central part of the fissure zone F_8 runs across a rice-field, giving vertical and horizontal displacements. Unusual ground water springs are also seen flooding on the down-thrown side. Some of these were associated with carbon-dioxide bubbles and chemical precipitates. Scales in the upper (a) and middle (b) of photographs are 1 m. Photograph taken Nov. 14, 1966.

a: Looking westward in the direction of the fissure zone. *En echelon* ground cracks define the zone.

b: Looking northward. Left-lateral offset of about 30 cm is indicated by the displaced rows of rice stocks.

just east of the area with nearly parallel trend of N55°~70°E. The vertical component of displacement is systematic in the two groups and it attains a maximum in the middle part of a fissure zone. The downthrown side is always to the north in the left-lateral group (Fig. 15) and vice versa in the right-lateral group. Movement in all the zones apparently stopped in the middle of September and thereafter showed slight north-south contraction.

As described in the first paper (Fig. 2), the occurrence of ground cracks is strongly controlled by surface geology, especially when the displacement is small. The most favourable place for ground crack formation is alluvial fans where a moderately dry surface soil layer

develops a metre or so thick. The surfaces of wet lowland seem to be too plastic for crack formation. This is the case, for example, around the hill where fissure zone F_4 is located. Steep mountain slopes also seem to be unfavourable for crack formation. Thus, F_6, F_{15}, F_{12}, for example, abruptly disappear when they are traced to mountain slopes from alluvial fans or talus slopes. Thus, the distribution of some fissure zones to a large extent is a function of surface geology and the zone fissuring may actually extend beyond the observable limits of cracking into the mountains and lowlands.

There are no topographic indications that these zones had displaced the ground prior to the present earthquakes, which means that these ground cracks have not formed recurrently in recent geologic time.

Additional remarks on individual zones

The most important features of the fissure zones are described in the previous section. Following is a case description along the entire length of zone F_1 and some additional remarks on other zones.

Zone F_1 includes the first reported ground cracks of A-type. As of April, 1966, the zone extended 275 m N80°W from a mulberry field about 35 m west of a road connecting Sezeki and Iwasawa. There, it consisted of scattered open cracks trending N70°E, several tens of centimetres in length and less than 5 mm in maximum separation. Only a single crack was encountered when the zone was traversed normal to its trend. A low stone-wall, similar to, but a little higher than, the one shown in Fig. 14 was collapsed where the zone intersected it at about 22 m from the eastern end.

West of the wall, an *en echelon* pattern of the cracks in the zone was quite clear. A few to several cracks up to a few meters long and maximum separations of a few centimetres were counted along the normal direction to the zone. A photograph (Fig. 4a in the first paper) shows the open *en echelon* cracks in this area. About half way along its length, the zone cuts two roads a few metres north of their intersection. On the EW running road any appreciable cracking was not observed, parhaps because it was newly built and gravel-surfaced. In contrast, the other road, which trends N35°W and had a firm well-packed surface, was broken by many ground cracks. 20～25 cracks were counted in 1.5 m normal to the direction of the zone. Each crack was a few tens of centimetres in length trending N60°～70°E or nearly perpendicular to the road, and had less than 5 mm of maximum separation.

West of the cross road there is a house, as shown in Fig. 5 of the

first paper. Locality F_1-a is in its garden. The appearance of a concrete slab crossed by the zone is illustrated in Fig. 6 of the first paper and in Fig. 13. Further to the west, there is a terraced field where ground cracks similar to those east of the cross road were observed. The western end of the zone was inside a house. The concrete foundation of the east side of the house was cracked at three points and opened 6 mm in total amount. On the inside extension of the largest crack (4 mm wide) a collapsed mud wall was noted. No damage was observed at the western side of the house, which has no concrete foundation. On the ground there were a few short cracks with trends similar to those of the fissure zone, but a definite distinction from ordinary dessication cracks was difficult.

By August 1966, all the fine structures of the zone on the ground surface had disappeared, except for the larger cracks. Instead, the zone became traceable by vertical displacement with the northern side downthrown. The vertical displacement took place along the zone, rather than along individual cracks. This is illustrated by Fig. 15a in zone F_8. The displacement, attaining about 30 cm in the central portion of the zone in Mid-September, is distributed across the entire width (less than 5 m) of the zone. The length of the zone also increased by about 15 m (Table 3) at the western end of the zone so that clear ground cracks were observed west of the house where they formerly terminated. In late August, outflow of ground water began at several places along the zone a few tens of metres east of the above-mentioned cross road.

The longest zone, F_5, has a peculiar feature in the arrangement of component cracks or in the sense of lateral movement. The middle and eastern part of the zone is similar to other zones, and the component cracks are uniformly arranged *en echelon*. The western part of the zone, trending in a direction of N80°E, consists of open cracks arranged parallel to the zone, bearing no lateral component of displacement.

Zone F_{13} was first visited by the writers only in March, 1967 guided by local residents. The ground cracks had already disappeared by that time, so that neither the sense of horizontal and vertical movement nor the pattern of ground cracks could be discerned. Observations by residents suggest that the zone is similar in dimensions to the other fissure zones. Its sense of lateral movement is not clear; it may be neutral, by analogy with the western part of F_5 which has the same N80°E trend.

Fissure zones F_{10} and F_{11} are located within about 10 m of the

landslides at Makiuchi and Kirikubo, respectively. Naturally, there are many ground cracks associated with the landslides that are invariably down-thrown on the downslope side, whereas F_{10} and F_{11} differ in that they are down-thrown on the upslope. But zone F_{11} at Kirikubo is not definitely decided to be of fault origin, because the first observation (February, 1967) of the zone was made after the landslide (September 25, 1966), when the original features were mostly destroyed.

Zone F_{14} consisted of a single continuous ground crack trending almost EW which coincides with a geologic fault. It obliquely crosses a narrow ridge in a N60°W direction. The north side subsided about 30 cm and no appreciable lateral slip was observed (Fig. 16). These features may not be explained as a simple effect of gravitational sliding, but might represent the result of displacement along a pre-existed fault plane due to earthquake vibration. As its distribution is isolated from other fissure zones, it is excluded in the following discussion.

Zone F_{16} was found by residents of Makiuchi under fallen leaves only on February, 20, 1967. It occurs on a steep slope of about 30°, nearly parallel to the maximum inclination. The *en echelon* pattern of component cracks indicates right-lateral displacement. The down-thrown side is on

Fig. 16. A ground crack crossing a narrow ridge (F_{14}). Relative subsidence of this side amounts to 30 cm. Looking south. Horizontal scale on the up-thrown side is 1 m. Photograph taken March 17, 1967.

the north. These features, which are comparable in orientation and sense of displacement with zones F_6 and F_{15}, are suggestive of a tectonic origin. However, the fault origin of the zone is not definitely established, because there are crescentic ground cracks enclosing the zone, which were found as early as September, 1966 (Fig. 11). There remains an alternative possibility that the zone were formed as the result of differential downslope movement. A similar explanation applies to the ground cracks shown in the southeastern part of Fig. 11.

3. Method of measurement

As described in the first paper, because the displacement of the ground cracks continued by creep after their formation, the writers tried to trace rates and directions of these displacements. Methods of measurement conducted at six localities on ground cracks and fissure zones are described in this chapter. The adopted methods were convenient for beginning frequent measurements as early as possible at additional localities. The first method was simple, but it was improved as new stations were successively added.

Simple methods were used where artificial structures—concrete slabs, concrete bases of wooden houses, concrete walls along ditches—traverse fissure zones, because the deformation of the ground is concentrated as a smaller number of distinct cracks in them. More elaborate devices were required in places without such structures.

The methods are classified into five types. Type I and type II$\sim$V were used, respectively, in the places with and without convenient artificial structures for measurement. All the methods were intended to measure the horizontal component of the displacement, because the vertical component had been negligible in earlier period, becoming significant only after the end of August, 1966. Therefore, the results obtained represent a close approximation to the actual horizontal displacement or represent displacement in the observation plane defined by reference points, the plane being inclined to small but various degrees by different methods and by different periods.

In the following description, the last suffix after each type (s, v, w) indicates methods using, two, three and four reference points, respectively.

Type Ia-s: Direct measurement of a gap in the ruptured artifical structure. Error of less than a few millimetres is unavoidable in most cases, because of the difficulty in finding exact corresponding points on each side of a gap.

Type Ib-w: This method was already described in the first paper[5]. Inverted nails are set in cement as reference points on opposite sides of a crack in an artificial structure, for example, a concrete slab (Fig. 17a). Four reference points are prepared to form a square with sides of about 15 cm across the crack (Fig. 17c). Displacements of points C and D relative to the base line AB in Fig. 17c are calculated by trigonometry, using values of distances AC, BC, AD and BD measured by ordinary rule to the nearest 1 mm. Difference of displacements between points C and D gives the amount of horizontal rotation of the concrete slab. This method inevitably results in error of a few millimetres in a direction parallel to the crack because of the inappropriate shape of a triangle set by three reference points. Later this method was improved into the following type Ic-w.

Type Ic-w: A vernier calliper is used instead of the ordinary rule for reducing the measurement error to the nearest 1/20 mm. As illustrated in Fig. 17b, reference points are made of screw bolts in lead tubes which are tightly inserted into the holes drilled in the concrete slab. The distance between centres of two reference points is given by subtracting the sum of radiuses of each bolt from the measured distance between outer sides of two bolts (Fig. 18). Otherwise, the procedure is the same as for type Ib-w.

Type Ic-s: Two reference points are used where available space is narrow (Fig. 19). The structure of reference points and the tool for measurement are the same as those in type Ic-w.

Type IIa-s: This method was used when no available artificial structures were found. Two concrete blocks are installed on the ground across ground cracks and an iron rod of 2.5 m long and 9 mm in diameter is laid over them.

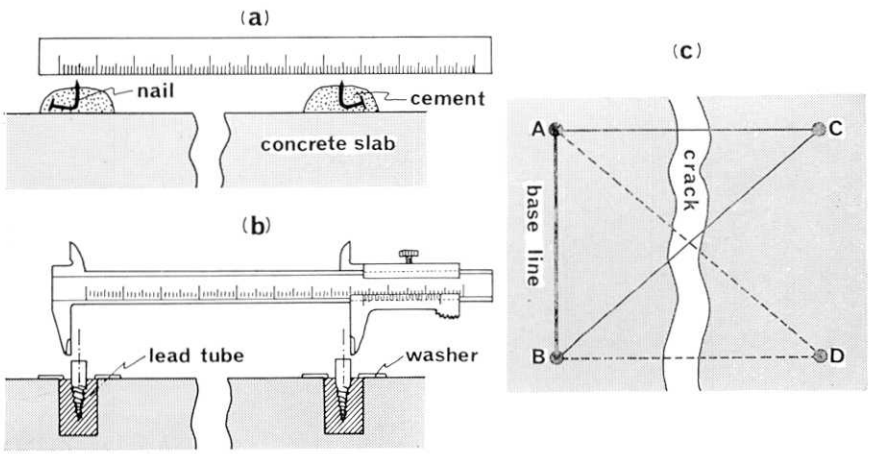

Fig. 17. Structure of reference points used in type Ib (a) and type Ic (b) and their arrangement (c).

5) K. NAKAMURA and Y. TSUNEISHI, *loc. cit.*, 2), p. 1377.

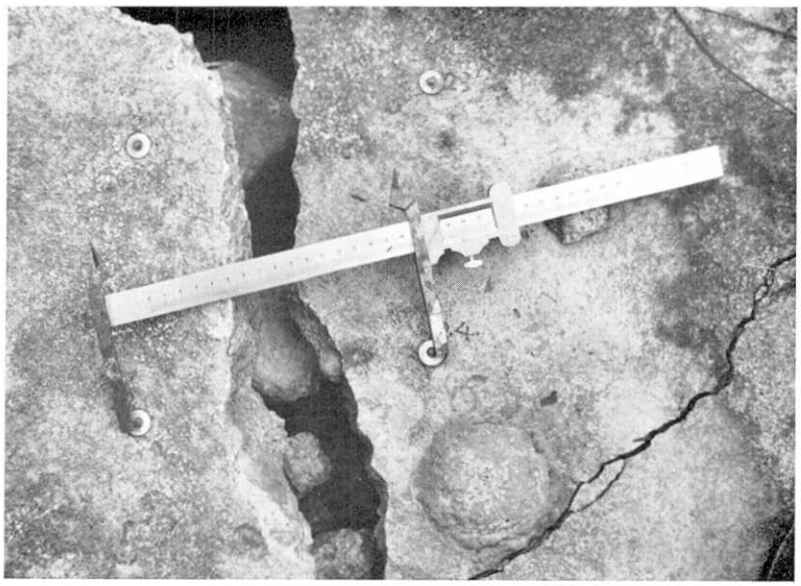

Fig. 18. Method of type Ic-w at Station F_1-**a**, D. The concrete slab on the left (north) tilted northwards by subsidence of northern side.

Fig. 19. Method of type Ic-s at Station F_2-**b** (**In**), where a crack occurred crossing a concrete base of a wooden house. Photograph taken Jan. 26, 1967.

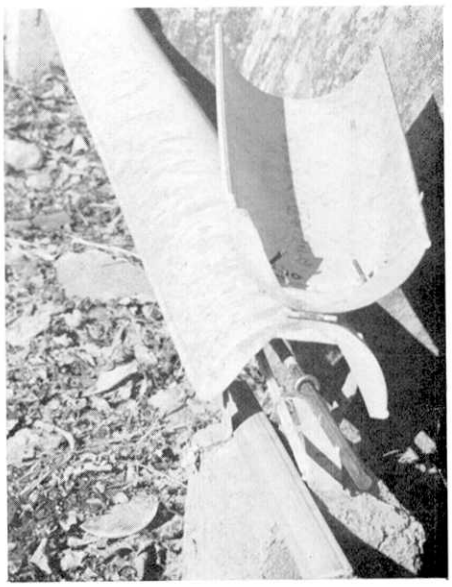

Fig. 20. Free end of type IIb-s installed on the road side at Station F_2-**c**.

A fixed end is supported by a vertical pin on the base so as to permit rotation of the rod around the pin, while the other free end is passed through a ring attatched to the base. Distance is measured by ordinary rule to the nearest 1 mm between the ring and the free end of the rod.

Type IIa-v: Two sets of equipments the same as type IIa-s are combined into a V-shape, in order to trace the displacement path.

Type IIb-s: To reduce thermal effects due to the change of atmospheric temperature, a sun cover is put over the rod and an appropriate temperature correction is carried out by a thermometer attached alongside the rod (Fig. 20).

Type IIb-v: This is type IIa-v improved by the above-mentioned attachment (Fig. 21).

Type III-v: Iron rod of type IIb-v is replaced by stainless steel pipe 2.5 m long and 19 mm in diameter with more elaborate fixed and free ends, to avoid bending and corrosion of the rod. A sun shelter is put over the pipe and a thermometer for temperature correction is inserted into the pipe. Two pipes are combined into a V-shape so as to observe the displacement path (Fig. 22). Distance is measured by vernier calliper to the nearest 1/20 mm between the ring fixed to the base and the free end of the pipe (Fig. 23).

Type IV-v: The automatic extensometer type IV was devised for increasing frequency of measurement and for decreasing the error. Invar wire 4 m long and 0.5 mm in diameter is used instead of a pipe or a rod. One end of the wire is fixed on the concrete base (Fig. 24), whereas the other end is attached to one end of the calliper main rule of a vernier calliper with the vernier fixed to the other base. From string attached to the opposite end of the main rule hangs a lead weight through a fixed pulley to put the wire under constant tension of

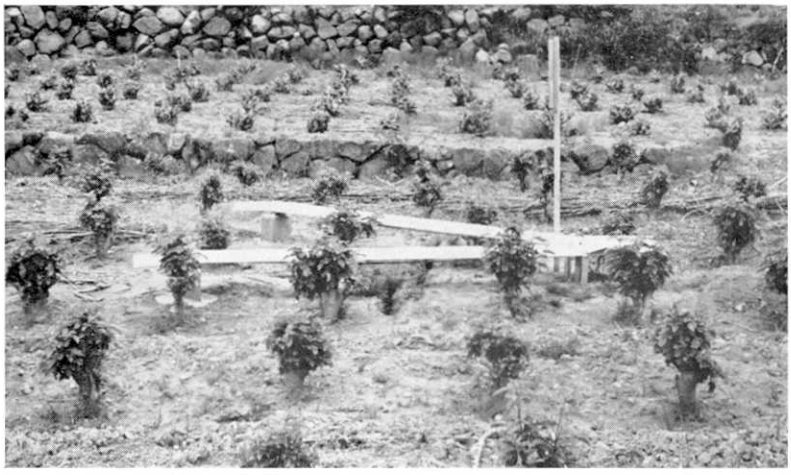

Fig. 21. Displacementmeter of type IIb-v installed in a mulberry field at Station F_3-**d**. Relation to ground cracks is shown in Fig. 28.

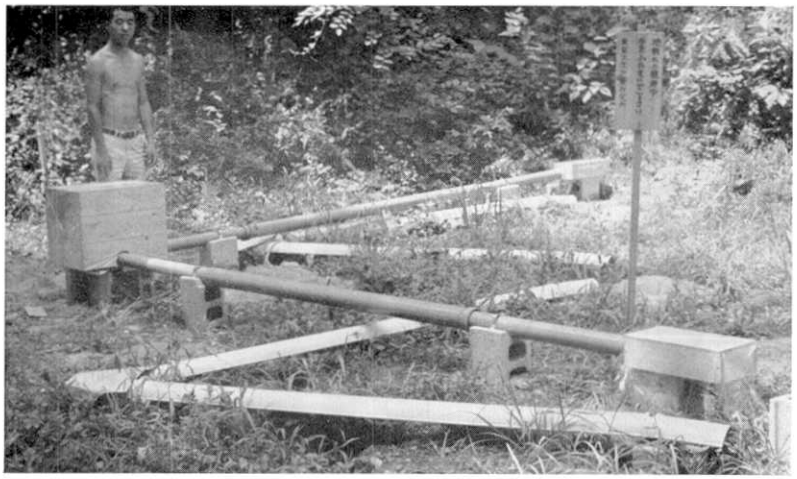

Fig. 22. Complete view of station F_4-**e** as seen from the east. Three sets of measuring instruments are installed, of which the smaller two are type III-v and the overlapping long one type IV. Relation to ground cracks is shown in Fig. 29.

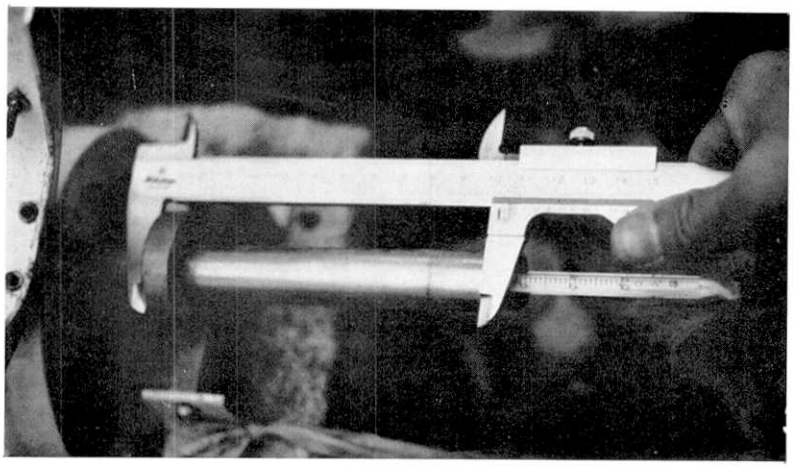

Fig. 23. Free end of type III-v under observation at Station F_4-**e**. A part of a thermometer inserted into a stainless steel pipe is seen (cf. Fig. 20).

about 1 kg (Fig. 25 and 26). The invar wire is passed through a plastic tube to protect it from direct sunlight and wind. Two sets of this extensometer are combined into a rectangular V-shape so that two vernier callipers are situated at the apex (Fig. 22). Over the apex a camera with automatic exposuring and film-winding device is set to photograph the two vernier callipers, a clock and a thermometer (Fig. 30). The shutter is actuated down by a solenoid coil into which electric current is sent from an electric timer at regular time

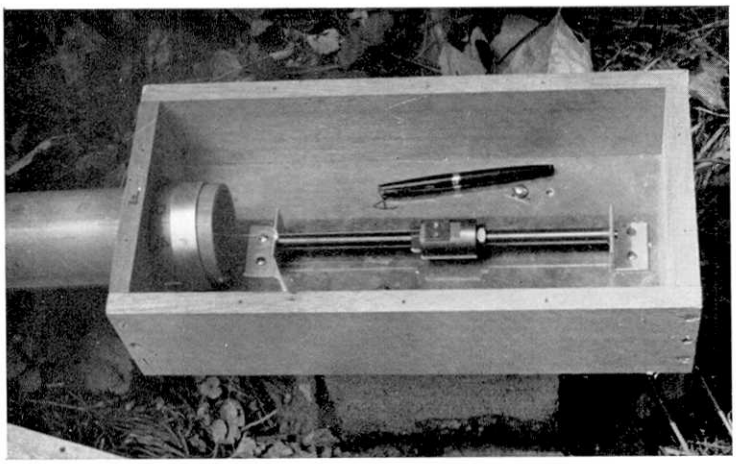

Fig. 24. Uncovered fixed end of type IV at station F_4-**e**. An invar wire is attached to a ring whose position is adjustable along an inner rod.

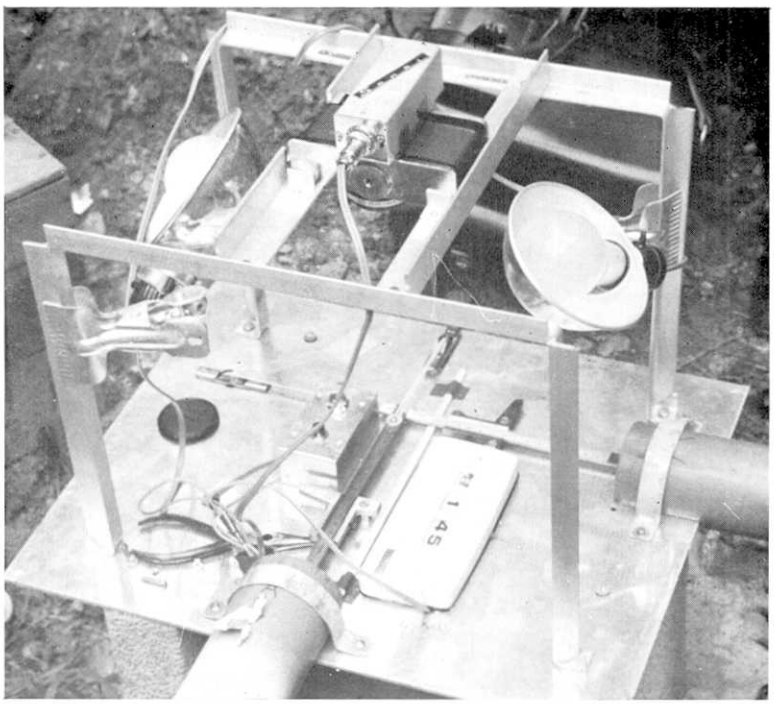

Fig. 25. Uncovered recorder of type IV. An automatic camera is positioned on the top.

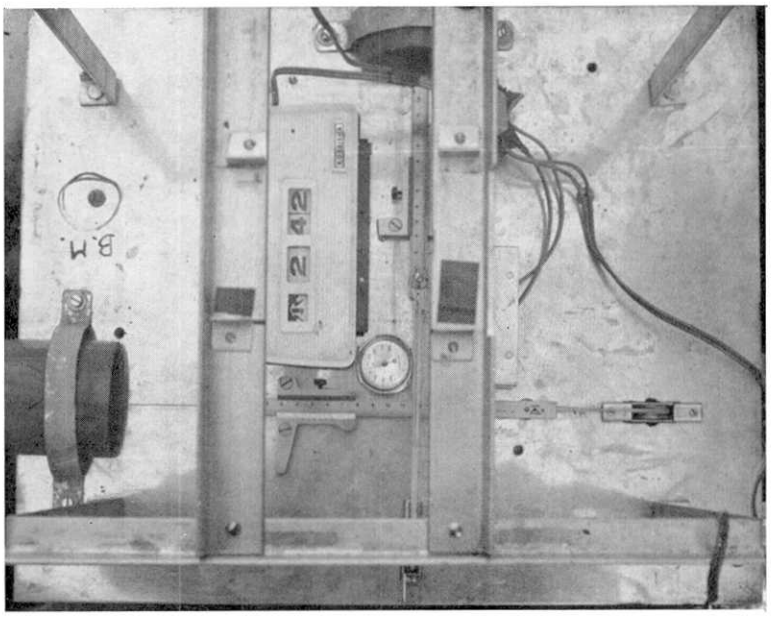

Fig. 26. Vertical view of instrument board of the recorder of type IV. Two vernier callipers, a clock and a thermometer are arranged. Automatic camera is removed.

intervals which can be chosen within the range from 1 sec to 24 hours. Photographs are taken by flash illumination in a dark box.

Type V: This method is used to detect the displacement of a whole fissure zone. Concrete blocks with reference points are installed on the ground and the distance between reference points is measured to the nearest 1 mm by a steel tape 20 m long under 5 kg tension. The measured value is appropriately corrected for atmospheric temperature changes.

4. Result of Measurement

General remarks

Measurements have been made once or twice a day at six stations (**a**～**f**, Fig. 12) on five fissure zones. Five of the six localities were also shown in Fig. 2 of the first paper. Methods of measurement at each station are listed in Table 4. Type Ia-s Ic-s and IIa-s give amounts of displacement only in a certain direction, whereas other methods give both paths and amounts of displacement.

Each displacement path illustrated in Figs. 32～41 represents a trajectory of a point on the southern block relative to the northern baseline.

Table 4. Type of method used at individual stations

Station	Start of measurement	Method	Related Fig. No.
F_1-a, AI, AII	Apr. 22	Ib-w (Apr. 22～June 21) Ic-w (June 22～)	5 17 27 32 33 42
F_1-a, DI, DII	Apr. 22	Ib-w (Apr. 22～June 21) Ic-w (June 22～)	5 17 18 34 35 42
F_1-a, BI, BII	May, 20	Ib-w (May 20～June 6) Ic-w (June 8～)	5 17 36 37 42
F_2-b, Ou	June, 21	Ib-s (June 21～)	17 42
F_2-b, In	May, 19	Ib-s (May 19～June 4) Ic-s (June 6～)	17 19 42
F_2-c	May, 19	IIa-s (May 19～June 8) IIb-s (June 12～)	20 42
F_3-d	May, 19	IIa-v (May 19～June 8) IIb-v (June 12～)	21 28 38 42
F_4-e, I	June, 10	III-v (June 10～Sept. 7)	22 23 29 39 42
F_4-e, II	June, 10	III-v (June 10～)	22 23 29 39 42
F_4-e, III	Aug. 9	IV-v (Aug. 9～)	22 24 25 26 29 30 40
F_6-f	Sept. 8	III-v (Sept. 8～) V (Sept. 9～)	23 31 41 42

The directions E-W and N-S are taken as axes of co-ordinates in the path diagrams and the values of the first measurement are plotted on the origin. Open circles connected with the origins by dotted lines indicate the inferred original position as estimated by the distance and direction between corresponding points on both sides of the cracks.

The amount of displacement regardless of direction is given by the distance from the origin to each point on the path diagram. The displacement-time curve for all stations are presented in Fig. 42. In the following paragraphs, the attitudes of ground cracks and fissure zones at each station are described and results of the measurements are given.

Individual results

F_1-**a**: The middle of the fissure zone F_1 traverses a house and its garden and displacement of the zone was measured in four cracks A, B, C and D on the concrete slabs (Fig. 5 of the first paper). Adopted method was originally type Ib-w and later Ic-w. Measurements on crack C were made for only a short period, because the crack was regarded as having formed by structural weakness rather than differential movement of the ground and also because its movement was relatively small. Displacement paths of the other three cracks are illustrated in Figs. 32～37. Diagrams classified as AI, BI and DI (Figs. 33, 35 and 37) represent displacement paths of the southwestern reference points among each four points relative to the northern base-lines, while AII, BII and DII (Figs. 32, 34 and 36) represent the paths of the southeastern points. As the vertical displacement gradually increased during August, making measurement difficult, two reference points on the down-thrown side of crack A were raised by 8 cm in September 4 (Fig. 27).

Exceptional features in displacement paths shown by diagrams DI and DII (Figs. 34 and 35) since September 19 are explained as the result of collapse of the ground under crack D thereby causing tilt of

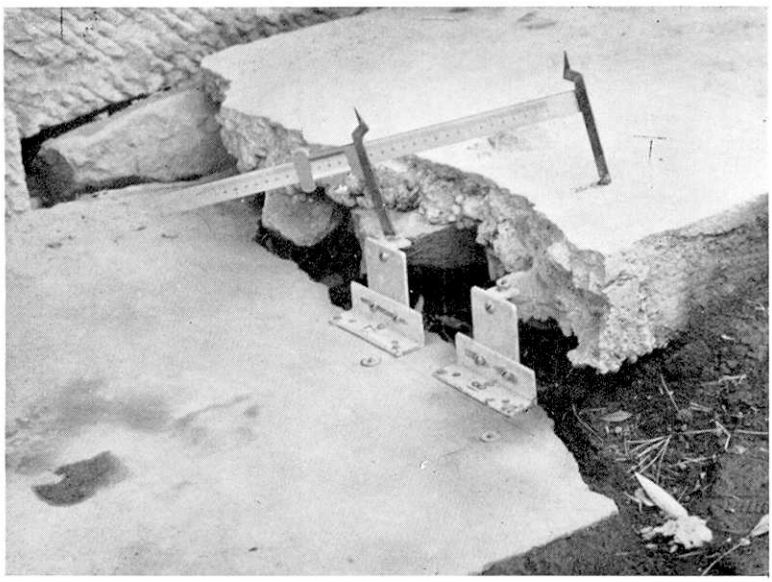

Fig. 27. Raised reference points of type Ic-w at Station F_1-**a** (A). Vertical displacement along crack A made the former measurement impossible. Photograph taken March 9. Vertical view is given in Fig. 13.

the concrete slab by about 30°. Gradual decrease of the ratio between opening normal to the crack face and lateral slip is indicated by gradual bending of the displacement paths of both AI and AII toward the east (Figs. 32 and 33). The same but slight tendency on DI and DII disappears from the middle of August, but this is interpreted as the result of additional opening caused by tilting of the fragmented slab at D which rapidly increased from that time (Fig. 18). Displacement of crack B is smaller and consists essentially of a simple opening.

The sum of displacement at cracks A and B represents the closer approximation to the total displacement across fissure zone F_1 at this station, whereas the result at D shows a smaller part of it, because the concrete slab covers less of the zone (Fig. 5 and p. 1377 of the first paper). Indeed, measurements at the end of March, 1967, of the distorted concrete slab as a whole, which had been a continuous square and was later broken by cracks A, B and C, gave about 17 cm north-south extension and 25 cm left-lateral displacement in an E-W direction. The indicated net displacement, therefore, is about 30 cm in a N55°W direction. This amount of horizontal displacement is nearly twice that of the sum of the measurement at cracks A and B because of the concealed amount by horizontal rotation of the fragmented piece of the slab.

F_2-**b**: At this station fissure zone F_2 ruptured the concrete base of a house in a direction N30°W at two points. Displacements have been measured by methods type Ia-s and Ib-s (Fig. 19). As the two cracks opened in a single concrete base across the entire zone, their sum represents the approximate amount of displacement of fissure zone F_2 at this place. F_2-**b** (**In**) showed exclusively extensional separation of about 2 cm while F_2-**b** (**Ou**) showed separation, left-lateral offset and vertical displacement amounting to 6 cm, 3 cm and 6 cm respectively.

F_2-**c**: Fissure zone F_2 crosses a road running in a direction N30°W. Displacement has been measured by method type II installed along the roadside (Fig. 20). The amount obtained at this station after August, 1966, represents approximately one half of the total displacement of fissure zone F_2, because another crack in the same zone appeared outside the coverage of the rod at the end of August.

F_3-**d**: Zone F_3 crosses a mulberry field where there are no convenient constructions for measurement (Fig. 28), and method type II (Fig. 21) was used. The measurement at this locality became impossible after the middle of September due to the submergence of the station and collapse and loosening of the soil under an extraordinary volume of

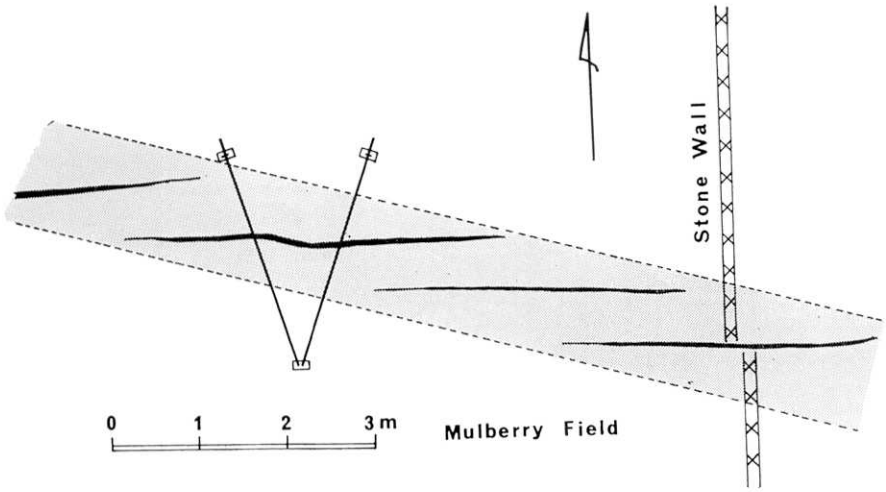

Fig. 28. Sketch map of Station F_3-**d**. Stippled area is the fissure zone F_3. A photograph of offset wall is given in Fig. 14.

water which welled out from the nearby ground. The displacement path (Fig. 38) shows a predominant strike-slip component. However the crack had already opened several centimetres before the beginning of measurement (Fig. 4b of the first paper) so that it is reasonably assumed that the opening-lateral slip ratio was larger during the earlier period. The last few points (extreme right) of Fig. 38 are regarded as being considerably affected by soaking of the ground with spring water. This also explains the exceptional curve of F_3-**d** in Fig. 42.

A nearby crack in the same zone trending in an E-W direction crosses a low stone wall at right angle. Offset of the wall indicates 20 cm left-lateral displacement, 10 cm opening,and 5 cm subsidence of the northern side (Figs. 14 and 28).

F_4-**e**: In this station fissure zone F_4 crosses the yard of a shrine on a hillside composed of Miocene shale and porphyrite. The ground cracks were judged to represent almost directly the movement of the bedrock. Thus a somewhat different pattern of displacement was anticipated from the foregoing stations all of which were on alluvial deposits. Measurement was carried out by extensometers of type III and IV whose position relative to the cracks are illustrated in Figs. 22 and 29. The plot of displacement paths (Fig. 39) also shows a prominent strike-slip component as observed in station F_3-**d**. A decrease of the opening-lateral slip ratio is also suggested here, because an opening

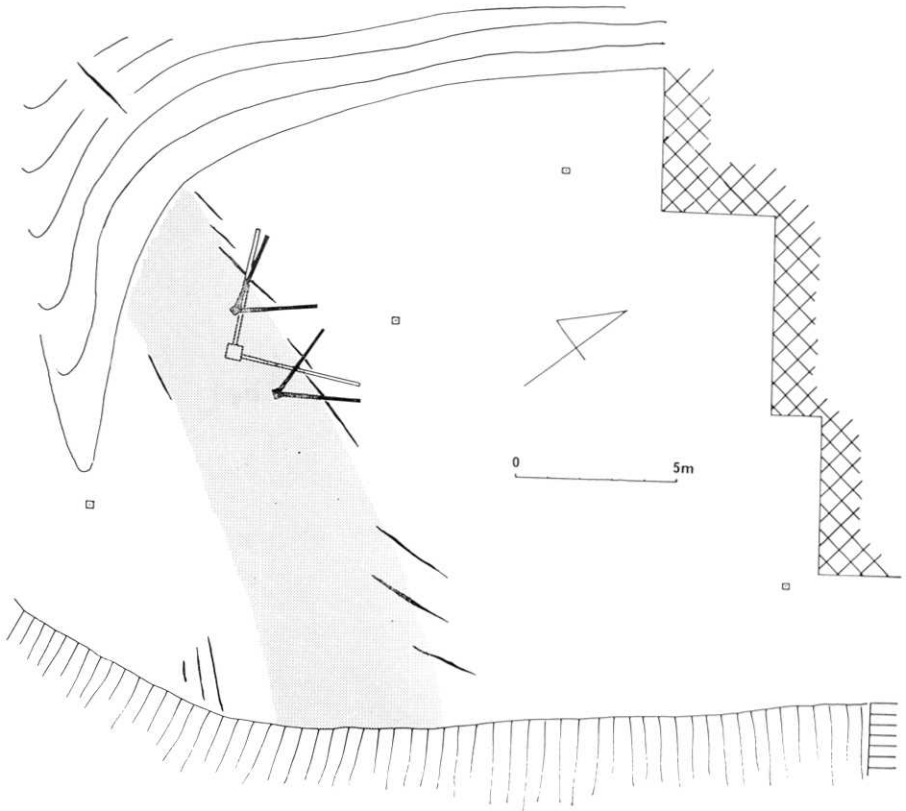

Fig. 29. Sketch map of Station F_4-**e** in the yard of a shrine. Three sets of measuring instruments are shown. Larger one is of type IV-v and the smaller ones are of type III-v. Stippled area is a graben-like depression of about 15 cm in depth developed in August and September, 1966.

of several centimetres had been observed prior to the beginning of the measurement. The time-displacement curve (Fig. 42) shows step-wise progress on August 20 and September 6 when two large shocks ($M=4.4$ and 5.0, respectively) took place, the epicentres being located on the extension of the assumed fault. A jump at August 20 is also recognized in the graphs at F_1-**a** (Fig. 42). The jump on September 6 was traced in detail by method type IV. The result shows that this jump did not occur in an instant but proceeded in several hours (Figs. 30 and 40).

F_6-**f**: This station is located in a wheat field (Fig. 31). The measurements have been carried out by displacementmeters types III-v and V. Reference points A, C and D which cover the whole fissure zone were used for the type V measurement and the displacement of point C relative

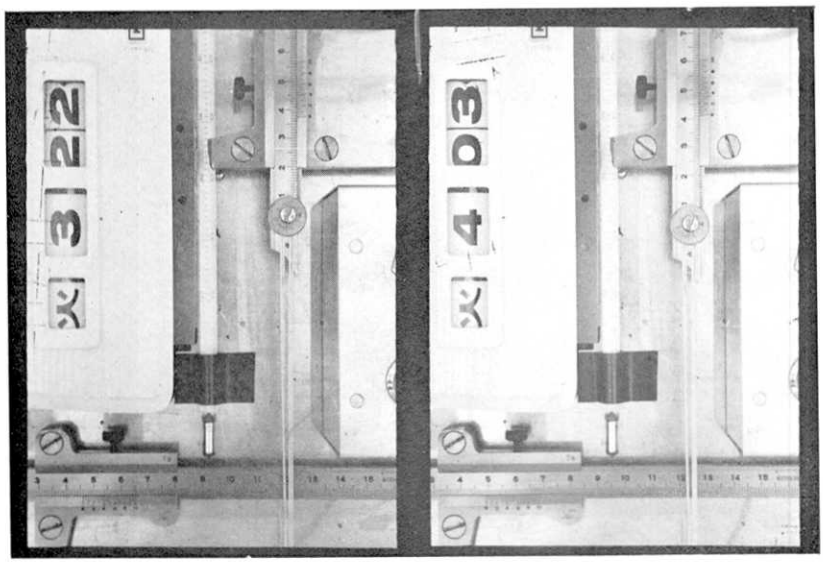

Fig. 30. Photograph taken by type IV just before (3 h 22 m) and after (4 h 03 m) a large shock (M=5.0, 3 h 37 m, September 6, 1966) recording an acute displacement. Lower callipers (NW-SE) show extension of 3.1 mm, upper ones (NE-SW) contraction of 3.7 mm, indicating lateral displacement during the 41-minutes interval between photographs. Analysed data are given in Fig. 40. The displacement may have taken place in far less than 41 minutes.

to base-line AD is illustrated in Fig. 41. The displacement path diagram reveals initial opening and succeeding right-lateral slip (Fig. 41). In Fig. 41 the points connected by solid and dotted lines are the results from type IV and V, respectively. The two graphs naturally show different amounts of displacement but are similar in shape. The measurement was begun about ten days after the formation of the cracks at this station* and a large initial amount of opening component was observed even though separation of 8 cm in a direction N15°E for the whole width of the zone was already apparent when the measurement started. In Fig. 42 (F_6-**f**) the upper graph connected by dotted lines represents the result of type V, and the middle and lower graphs connected by solid lines the results of type III. As the displacement path by type III shows a sharp bend at point M (Sept. 12, 1966) in Fig. 41, the amount of displacement is represented in two ways; the distance between each point and the origin (lower graph) and the distance between the origin and M plus between M and each point (middle graph).

* Because the displacementmeter (Type III-v) already set at F_4-**e** was made use of here, the time required for setting up the instrument was reduced.

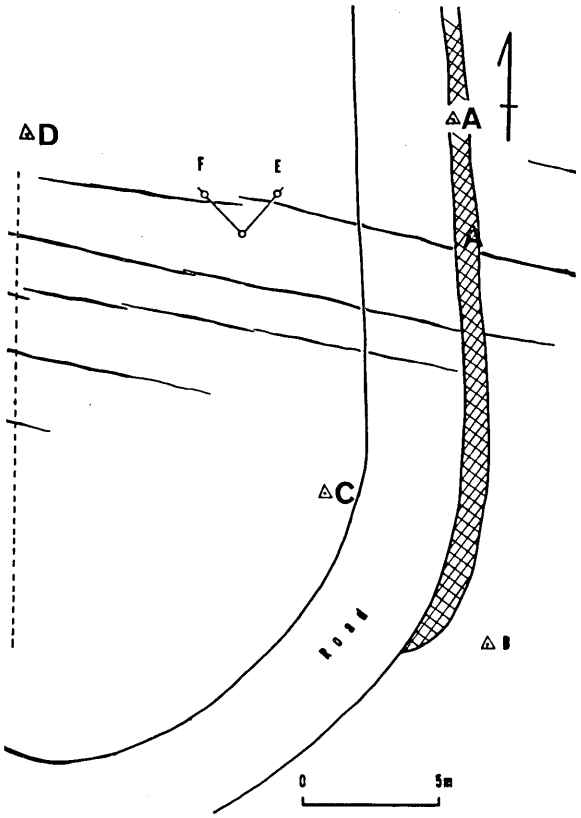

Fig. 31. Sketch map of Station F_6-**f**. A, C and D are reference points used by a method of type V. E and F are free ends of type III-v.

Summary

1. The time rate of horizontal displacement bears a striking similarity at all stations regardless of the degree of coverage of the fissure zones (Fig. 42).

2. Two periods of high displacement rate are recognized in April-May and August-September, 1966 coinciding with the period of high seismicity period. The amount of displacement in the latter period attains 1.5 times that of the former (Fig. 42).

3. Between the two active periods only a small amount of displacement proceeded. The amount is exceptionally large at station F_4-**e** (Fig. 42).

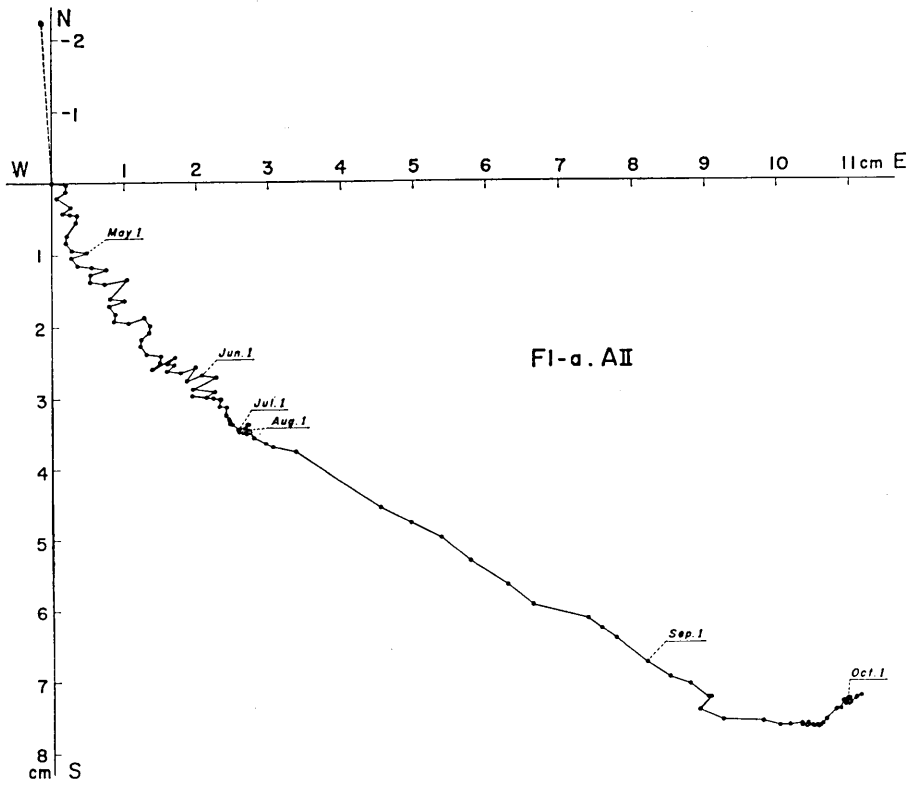

Fig. 32. Displacement path of the southeastern reference point observed at Station F_1-a (A). Earlier part of this plot was given in Fig. 8(II) in the first paper.

4. After the last active period a slight contraction in a N-S direction is observed as shown in the diagrams of displacement path (Figs. 32, 33, 36, 37, 39 and 41).

5. At station F_4-e distinct jumps in displacement of about 1 cm took place, corresponding to two large shocks located on the extention of the assumed fault (Fig. 39). These jumps took place over a period of several

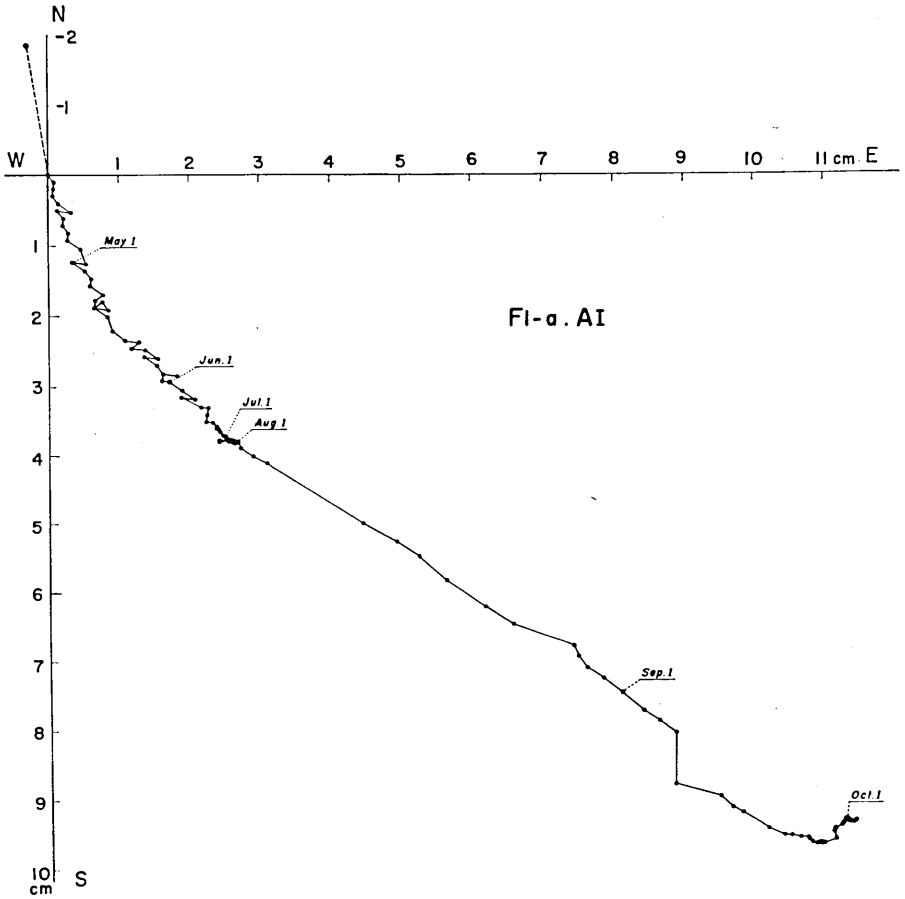

Fig. 33. Displacement path of the southwestern reference point observed at Station F_1-**a** (A). Earlier part of this plot was given in Fig. 8(I) in the first paper.

hours (Fig. 40).

6. In the earlier period of their developement, horizontal displacement of the ground cracks seems to be larger in the opening component, while in the later period they were larger in their lateral-slip component (Figs. 41, 32 and 33).

7. No specific data of vertical displacement is available. However, it apparently took place in August, 1966 and since then it progressed keeping pace with the horizontal displacement. The downthrown side

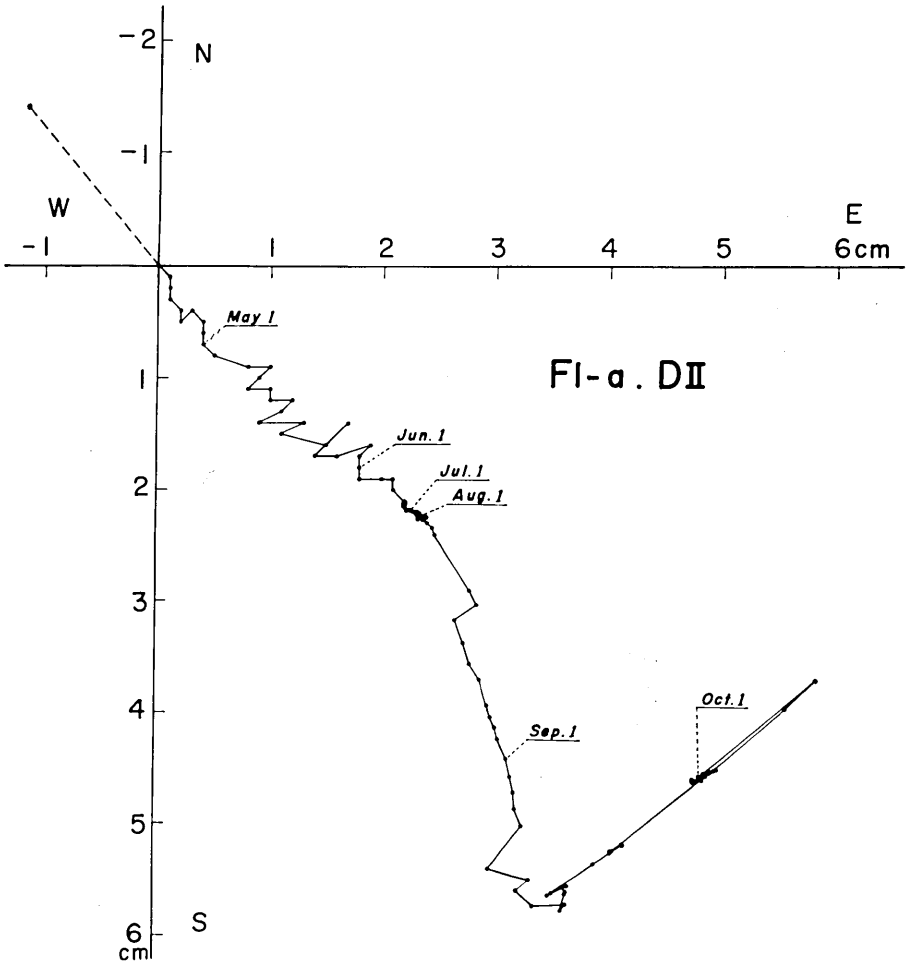

Fig. 34. Displacement path of the southeastern reference point observed at Station F_1-a (D). Earlier part of this plot was given in Fig. 9(II) in the first paper.

is south as to the right-lateral zone F_6, whereas it is north as to other stations on the left-lateral zones, as described earlier (Table 3).

Among the above-mentioned statements, 3 and 5 will point to the possible plastic mode of response to stress of unconsolidated surface deposits. F_4-e is the only place where unconsolidated deposits (actually talus debris) are negligibly thin and the observed displacement will be regarded as nearly representing movement of indurated rocks. Then the interpretation for 3 and 5 will be that both earthquake-related and creep

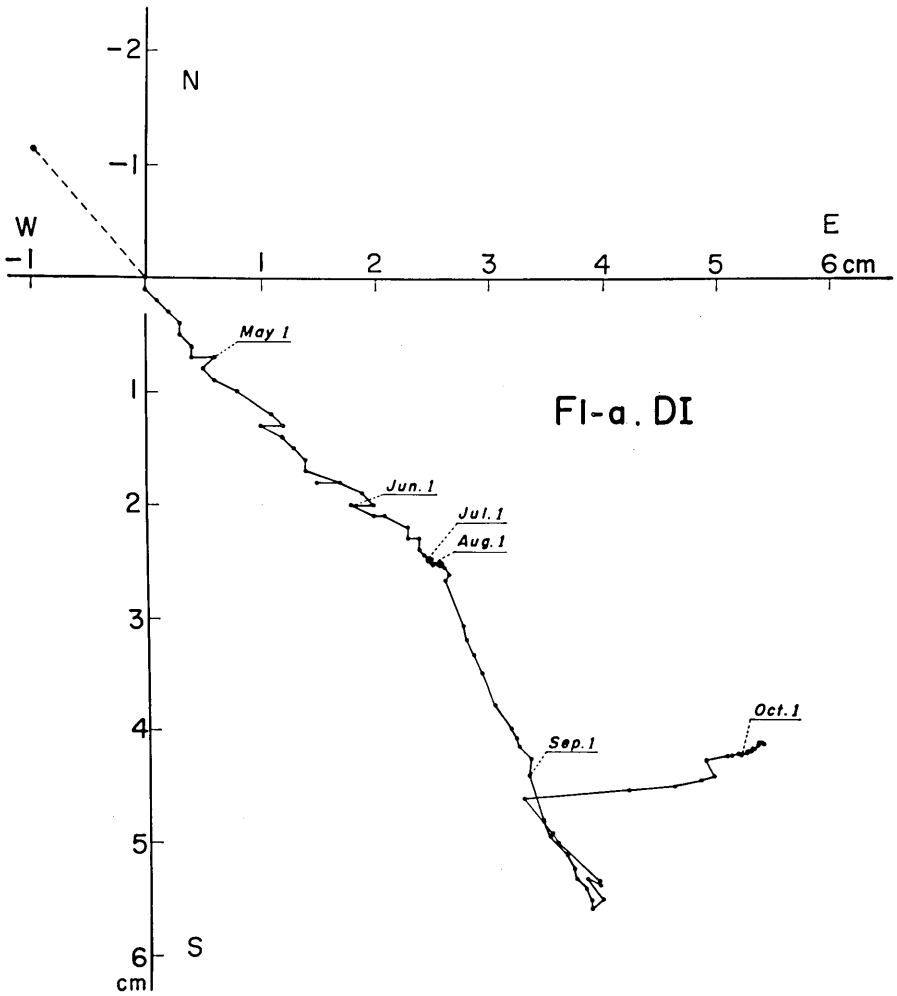

Fig. 35. Displacement path of the southwestern reference point observed at Station F_1-a (D). Earlier past of this plot was given in Fig. 9(I) in the first paper.

displacements in the base rocks were better observed on the ground where the unconsolidated cover is negligible. The plastic response to stress of unconsolidated layers is also suggested by the comparison of ground crack displacement with the result of electro-optical measurements (Fig. 49).

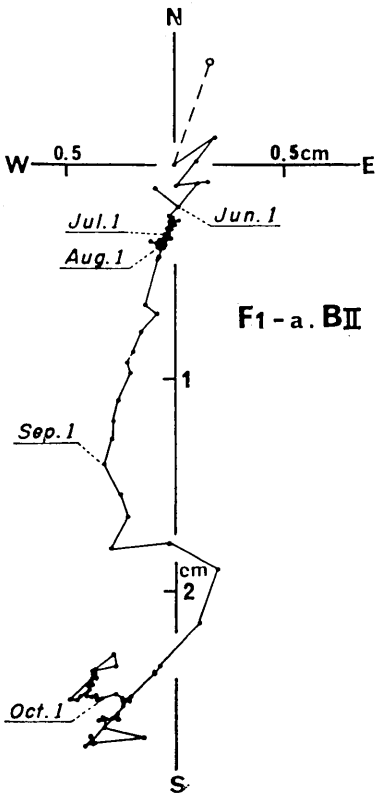

Fig. 36. Displacement path of the southeastern reference point observed at Station F_1-a (B).

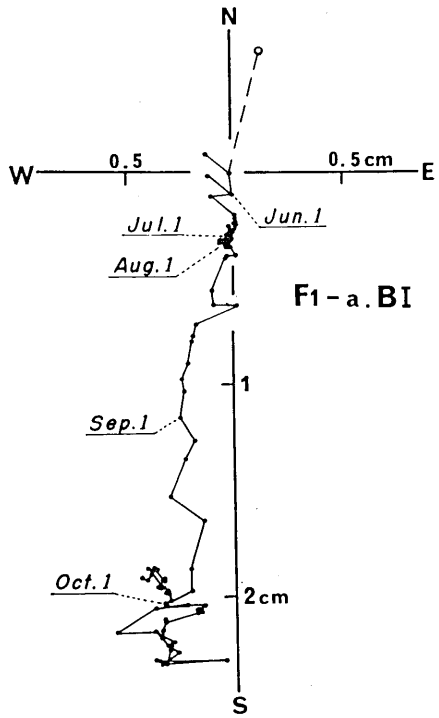

Fig. 37. Displacement path of the southwestern reference point observed at Station F_1-a (B)

5. Field observations on the NW extension of the fissured area

Open cracks in levees (ridges between rice-fields)

Northwest of F_4, there stretches a flat alluvial plain used for rice-fields (Fig. 11). Individual rice-fields are bordered by levees made of either mud or concrete (Fig. 43a). The concrete levees are useful for detecting zones of ground deformation.

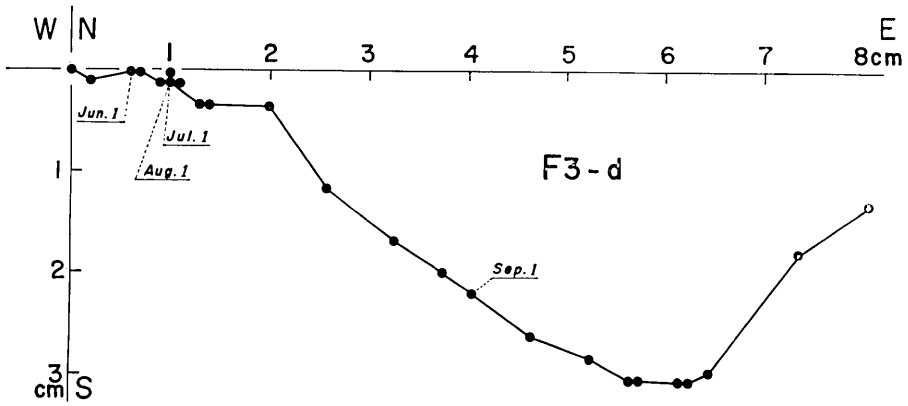

Fig. 38. Displacement path at Station F_3-**d**.

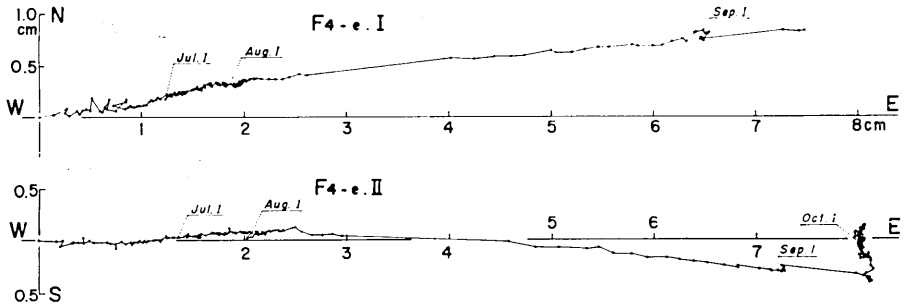

Fig. 39. Displacement path by type III-v at Station F_4-**e**. I and II are the results of the eastern and the western sets, respectively (Figs. 22 and 29).

In Fig. 44, the levees are shown by solid lines, among which the thick lines indicate those made of concrete. Most of the levees are oriented in N-S (N10°W, strictly speaking) and E-W directions and are a few tens of metres in length. While no deformation is observed in levees of mud, many open cracks up to 6 cm without any appreciable lateral offset, are found along concrete levees trending in a N-S direction. Cracks less than a few mm per 10 m are also found in concrete levees in an E-W direction, but almost all of them are not opened and show no displacement.

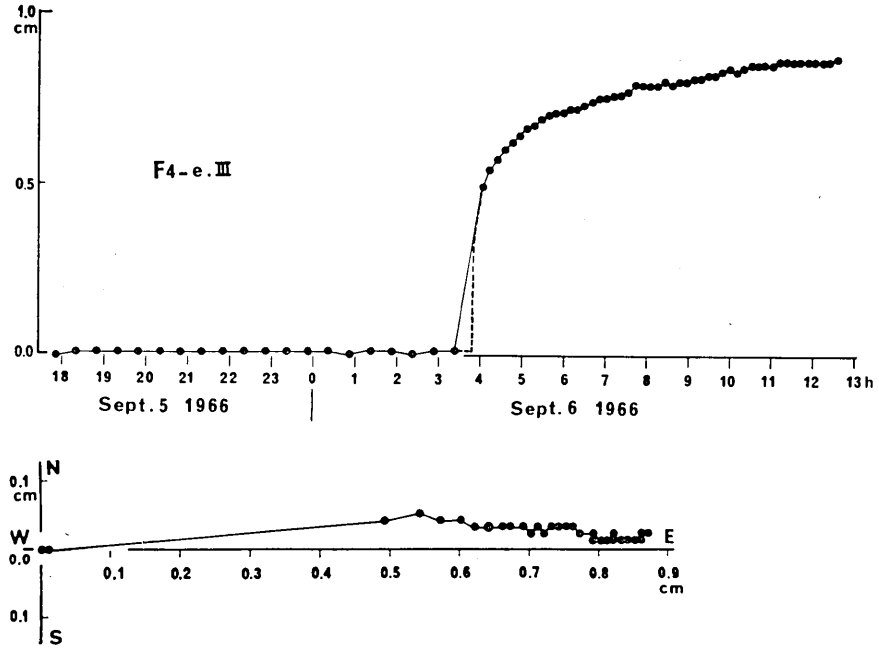

Fig. 40. Displacement path (below) and amount of displacement (above) before and after a large shock (M=5.0) observed by type IV at Station F_4-e.

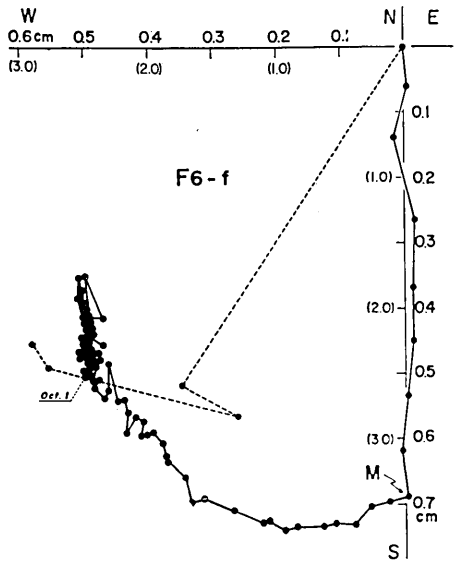

Fig. 41. Displacement path observed at Station F_6-f. Results by type III and type V are represented by solid circles connected by solid and dotted lines, respectively. Scale for the latter is parenthesized.

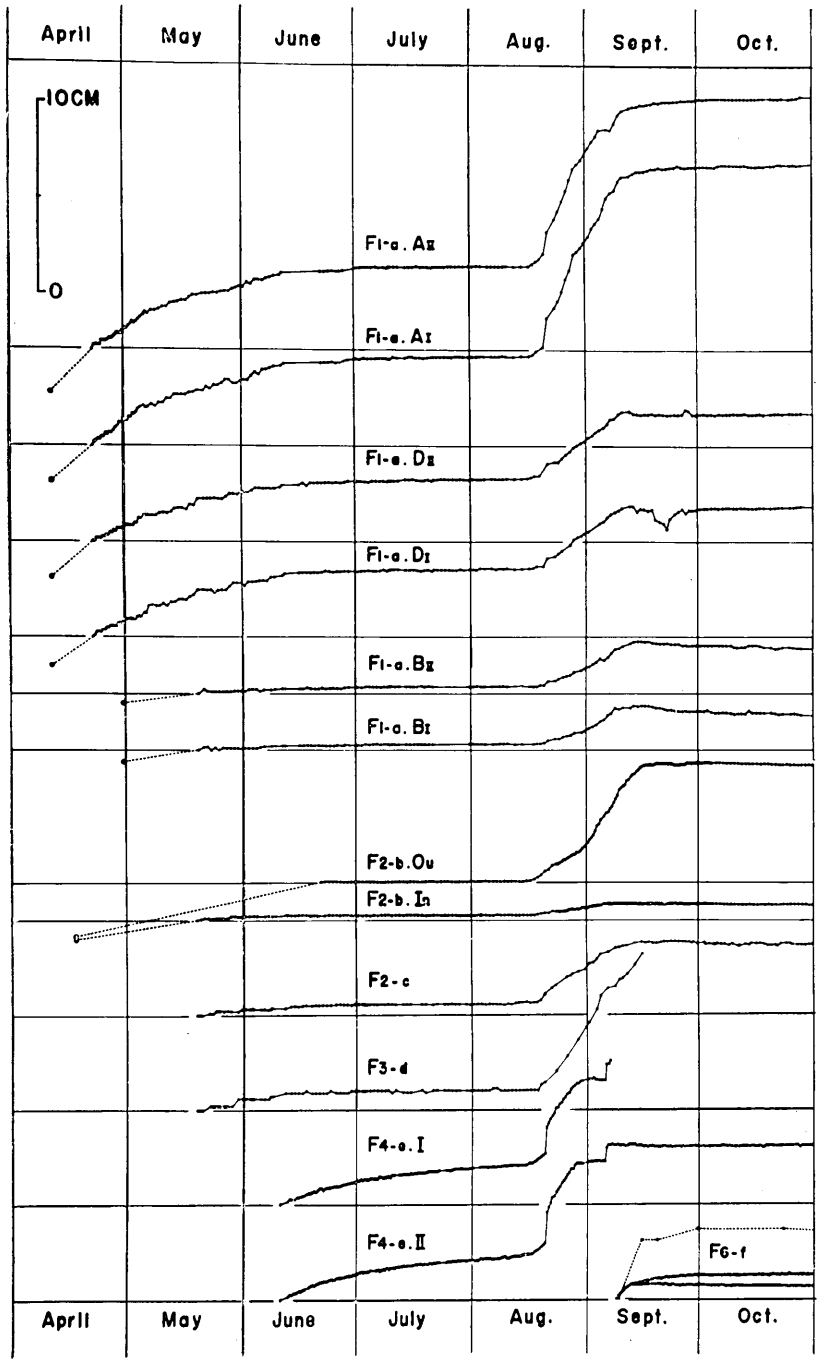

Fig. 42. Amount of displacement at all stations, prepared from Figs. 32~39 and 41.

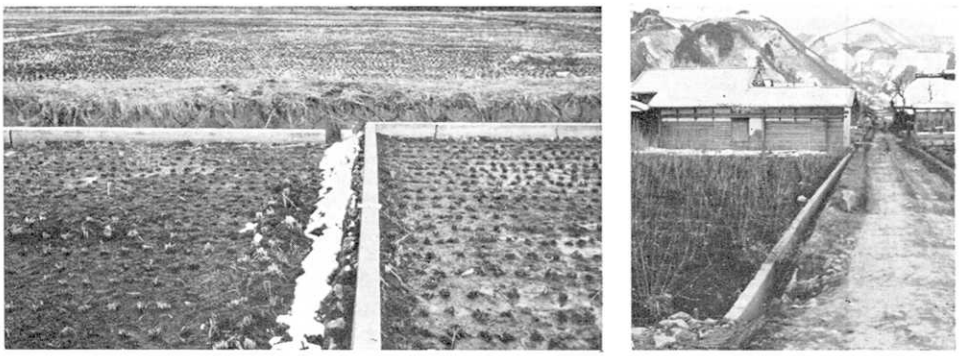

(a) (b)

Fig. 43. a: Cracks in concrete levees between rice-field, looking eastward. Note that there are three open cracks in the levees in a N-S direction whereas the E-W levee is free from cracks. Photograph taken Feb. 21, 1967.
b: concrete side-ditch dealt with in Fig. 46. Photograph taken Feb. 21, 1967.

The amount of separation of cracks in concrete levees in a N-S direction is shown by contour lines in Fig. 44 in units of mm per 10 metres. The upper figure shows the results of measurement on July 17, 1966 and the lower one, September 7, 1966. The separation shown in the westernmost part of the lower figure was measured along a concrete side-ditch on September 16, (Fig. 46).

According to owners of these rice-fields, these cracks became noticeable during April and May, 1966. From the comparison with the two maps, it is evident that the deformation is concentrated in a narrow belt trending northwest and that it progressed in the same area between the dates of the two measurements. The apparent opening in a north-south direction indicates the left-lateral sense of movement along the belt.

The southeastern extension of the axis of the belt passes some fifteen metres south of the triangulation point, 393,66 m (Fig. 44). This fact is significant when the result of triangulation is later discussed (p. 463).

Deformed railroad track

North of the town of Matsushiro, there is a slightly deformed railroad track originally running straight in a direction N20° E. The deformation consists of abnormal elongation, left-lateral offset and vertical displacement.

The Kato line of the Nagano Electric Railway Co., Ltd. consists of a single track and its location in the Matsushiro area is shown in Figs. 10 and 12. The track northeast of the Matsushiro station conforms

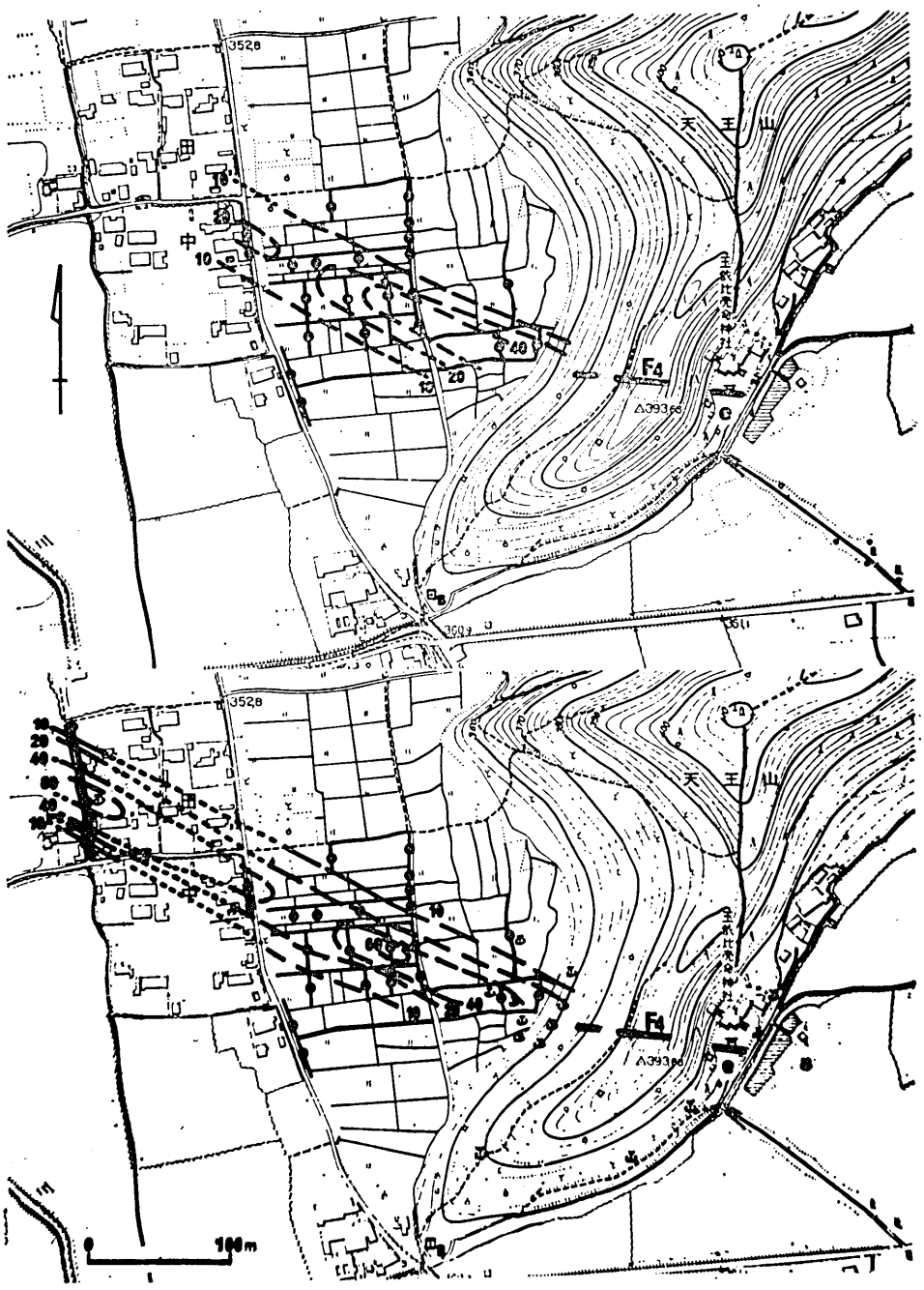

Fig. 44. Opening deformation of levees (ridges between rice-field). Thick lines indicate levees made of concrete, thin ones of mud. Unit in millimetre per 10 metres. Upper figure, July 17, 1966, lower September 7, 1966. In the lower map, localities of new springs started toward the beginning of September are also indicated.

to a straight line, trending N20°E, for approximately eleven hundred metres. The track is built on the flat aluvial plain which is an abandoned stream course of the Chikuma river. Most of the area has been used for farming mulberry trees, and is underlain by thick unconsolidated Quaternary sediments. The exact thickness of the sediments is not known but it is estimated to be more than several tens of metres from the comparison with the data of adjacent areas. An electric resistivity survey[6] of this area found a low resistivity layer of about 200 m

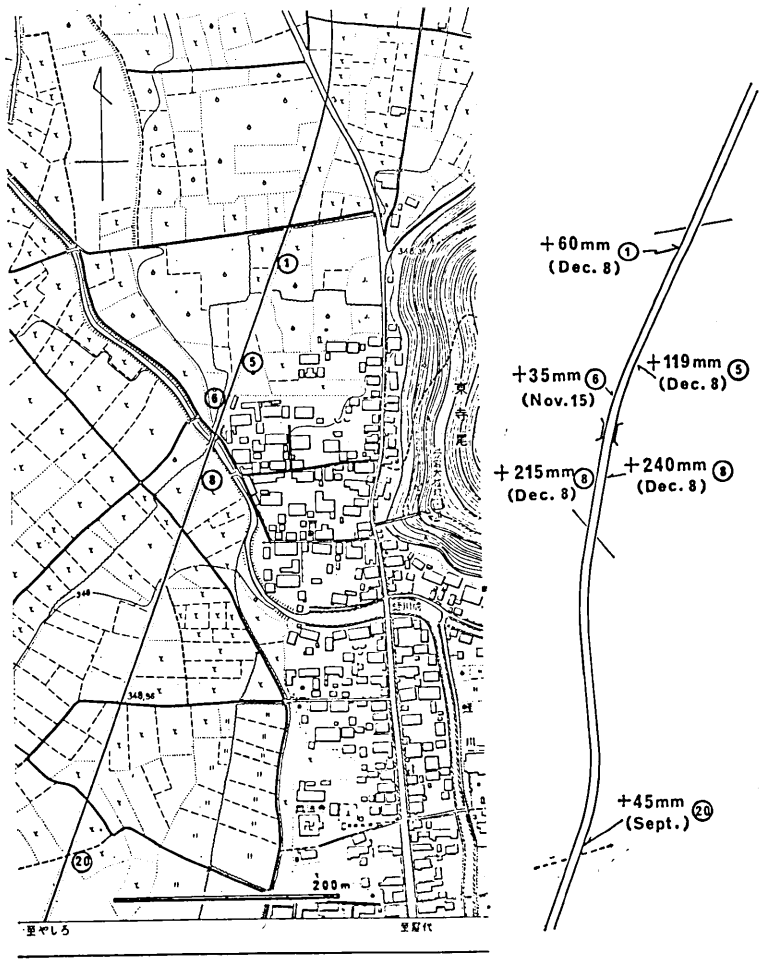

(a) (b)

6) SEYA, K., *Geologic News* (*Chishitsu Nyūsu*) No. 149 (1967), 17, (in Japanese).

(c)

Fig. 45. Deformation of a railroad track.
a: locality of the railroad and the position and specific number of replaced rails.
b: exaggerated expression of the deformed track, the increment of rails by replacement and their positions and dates are given.
c: photograph showing the deformation of the track, looking north.

thick (less than 20 Ωm) below the surficial layer of about 50 m thick (a few hundred Ωm) under the railroad track. Below the low resistivity layer, there is a high resistivity layer (about 1000 m) which consists possibly of Miocene intrusives.

The deformation of the track, as observable with the naked eye is shown, somewhat exaggerated in Fig. 45b. An instrumental survey has not been made of the railroad line. According to personnel responsible for track maintenance, the bending was noticed in April, 1966 and further increased during August and September of the same year. Bending was accompanied by increased clearance of joints between rails and breakage of bolts severe enough to require repair work. The deformed track consists of, roughly speaking, two parallel lines and an oblique intermediate part. There are three bending points with an additional one in the oblique part. Thus, during September the east-side rail of the southern bend was replaced by one which is 45 mm longer than the old one. Next, in November the west-side rail of the northern bend was

replaced by a 35 mm longer rail. Overall readjustment was undertaken in December replacing four rails by longer ones in the area under study. The estimated amount of the lateral offset by naked eye observation ranges between 200～500 mm from different base-lines. It is interesting to note here that in March, 1965, prior to the Matsushiro earthquakes, offset of 300～200 mm was already noticed by maintainance personnel when looking southward from the northernmost cross point of the track with the street as shown in Fig. 45a. The same person who noticed the preseismic offset also noticed an additional offset after the beginning of the earthquakes amounting to 200～300 mm looking from the same point.

Vertical displacement is also apparent by careful naked-eye observation from distant places as shown in Fig. 45c which was taken at the southern extremity of Fig. 45a·b. Although the change of level is very gradual, it is clear that the northern side of rail No. 20 has subsided by a few tens of centimetres.

From the above information, it is apparent that a consiberable part of the deformation occurred in relation to the present earthquakes, but

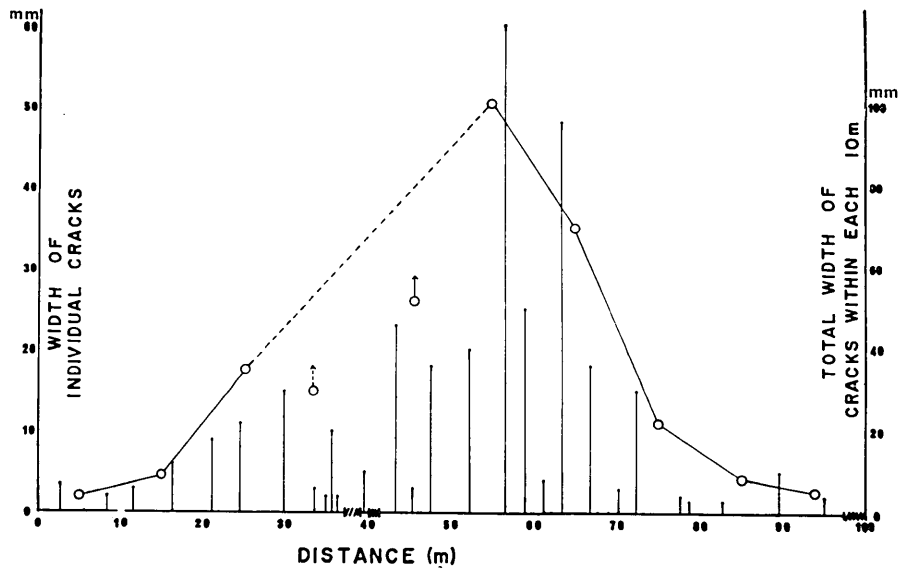

Fig. 46. Distribution of open cracks along a roadside ditch. Vertical lines indicate the location and separation of individual open cracks. Open circles represent accumulated sum of separation for each 10 metres. Hatched parts of the horizontal line show the places where the concrete ditch is either discontinuous or incapable of being observed due to obstacles.

there also were creep offsets before the earthquakes. The most recent deformation proceeded together with an unusual extension of the ground in the direction of the track, which coincided with the active period of the earthquakes.

Open cracks in a roadside ditch

Measurements along a roadside ditch (Fig. 43b and western extemity of the lower map of Fig. 44) provide data on extension of the ground in a N10°W direction. The ditch was constructed about 10 years ago and no wide open crack was noticed up to 1966. A number of open cracks without appreciable lateral offset are distributed in the ditch at present (Fig. 46). The ditch about 100 m long was originally separated in two points about 40 m from the northern end. In Fig. 46, both the individual amount of separation and sum of these values for each 10 m on September 16 are presented in terms of horizontal distance (measurement by type Ia-s). Gaps of the cracks are symmetrically distributed in a manner similar to that of the deformation of levees in

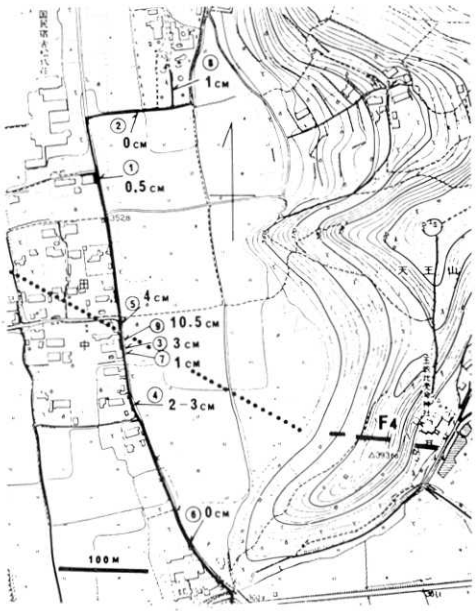

Fig. 47. Location of damaged water pipe to Ichiyōkan Hotel. Thick line shows the water line. Arrows indicate positions of damage, and distances pulled apart by the damage. Numbers in circle are common to those in Table 5.

Fig. 48. Photograph showing the pull apart damage of a water pipe in shallow underground. Number 9 in Fig. 47 and Table 5. The distance is 10.5 cm. Photograph taken by Mr. Isao Kasuga, on September 9, 1966.

nearby rice-fields to the SE. The simple sum of the crack separations amounts to 324 mm.

Damage to an underground water pipe

An underground water pipe running approximately N10°W between the above-mentioned ditch and the rice-field (Fig. 44) also indicates the ground extension in that direction associated with the present earthquakes. Location of the pipe and amount of opening are shown in Fig. 47. Nine ruptures occurred in 1966; the dates of breakage or repair are listed in Table 5. The ruptures were nearly always a simple pull apart at joint connections between drawpipes an inch and a half in diameter (Fig. 48). The damage was concentrated in the belt of strong deformation defined by the levee and ditch deformation. No appreciable amount of differential movement has been noticed between the pipe and the ground both at the southern end in the Fig. 47 where the pipe appears on the surface and at the northwestern angle. The sum of the openings, 22~23 cm, is an approximation to the total extension. It may be somewhat smaller, however, because there is possibly an additional breakage that was not discovered*.

Table 5. Dates of breakage and length of separation of water pipes

loc. no.	Dates of		length of separation (cm)
	breakage	repair	
1	?	1966 Jan. 13	0.5>
2	1966 Apr. 11	Apr. 11	0 (slight lateral displacement)
3	?	May 11	3
4	?	May 11	2-3
5	?	May 12	4
6	?	May 29	0
7	May 28?	May 29	1
8	May 28	May 29	1
9	Aug 28?	Sept. 9	10.5

(Data after Isao Kasuga, personal communication)

6. Examination of Fault origin hypothesis

Diverse evidences which support the buried left-lateral strike-slip fault origin hypothesis for the interpretation of the fissure zones of A-type (Fig. 12 and Table 2) are summarized in this chapter.

It will be accepted from the description of fissure zones in chapter

* After Mr. Isao KASUGA, the owner, personal communication.

2 and discussion in the first paper (p. 1382) that the A-type fissure zones are not to be attributable to simple upheaval of the ground nor to down slope movement of the ground (or landslide in a broad sense).

On the other hand, common origin of these fissure zones are strongly suggested by

1. quite similar time rate of displacement (Fig. 42) at six different stations despite their scattered distribution and various degrees of coverage of zones,
2. systematic horizontal and vertical displacement along the zones (Table 3),
3. uniform trends of component cracks regardless of sense of lateral displacement of the zones (Table 3),
4. uniform trends of fissure zones in the left-lateral and right-lateral groups (Table 3).

The time rate of displacement in the fissure zones are not only

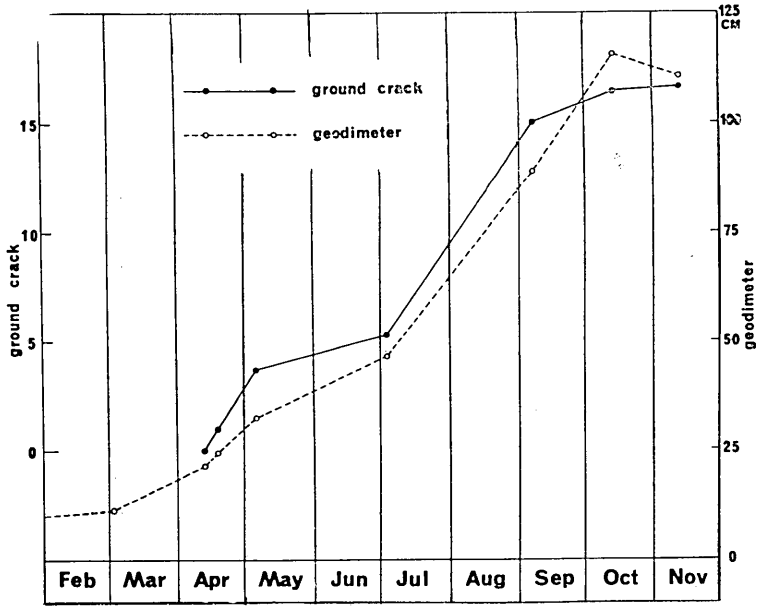

Fig. 49. Comparison of the time rate of displacement. Solid circle: measurement across a ground crack, at F_1-a (Fig. 12), simplified from F_1-a-AI in Fig. 42. Open circle: electro-optical mesurement along a base line about 3 km long, between Mt. Minakami and Sorobeku (Fig. 12).

7) K. KASAHARA and A. OKADA, "Electro-Optical measurement of Horizontal Strains Accumulating in the Swarm Earthquake area (2)", *Bull. Earthq. Res. Inst.*, **45** (1967) 272.

similar to each other but also to the result of electro-optical measurement between Mt. Minakami and Sorobeku[7], about 3 km long and in a direction of about N10°W (Figs. 12 and 49). The result by geodimeter represents the variation of horizontal distance between the two stations in a fixed direction, while the ground crack data represent the distance between two reference points in different directions. When the ground crack data in a N10°W direction are taken, contraction during late September and October is clear (Figs. 32–39 and 41), and the similarity between the two curves will increase. This striking similarity may indicate that the mode of displacement of fissure zones with time reflects a regional pattern of deformation. The high rate of displacement including the initial formation of ground cracks also agrees well with the two culminations in seismicity during April to May and August to September, 1966. Moreover, there is an intimate relation between the high-rate of displacement and larger shocks which occurred under the extension of the fissured area.

A buried left-lateral fault hypothesis is able to explain all the foregoing evidences. Moreover, it explains that the left-lateral fissure zones arranged *en echelon* are distributed in a narrow area and that comparable phenomena to ground cracking are observed, such as the deformation of a railroad track (Fig. 45), water pipes (Fig. 47) and concrete levees (Fig. 44) on the northwestern extension of the area. The hypothesis is consistent with the systematic distribution of the first P'polarity of the major[8] and micro[9] Matsushiro earthquakes, in that it assumes an accumulated maximum compression in an E-W direction as discussed in the first paper (p. 1382).

A most conclusive support to the hypothesis was given by the result of triangulation over the epicentral area conducted by the Geographical Survey Institute[10] (Fig. 50). The results of this survey suggest a left-lateral displacement along a line in a NW direction running through the northeastern foot of Mt. Minakami.

Fissure zones with a right-lateral sense of displacement which are distributed outside along the area of left-lateral zones, may possibly be a manifestation of a buried right-lateral fault or faults which is

8) M. ICHIKAWA, "Statistical Study of the Focal Mechanism of Matsushiro Earthquake Swarm", *Jour. Seism. Soc. Japan*, **20** (1967), 116 (in Japanese).

9) The Party for the Seismographic Observation of Matsushiro Earthquakes and the Seismometrical Section, *loc. cit.* 1).

10) Geographical Survey Institute, "Report of geodetic survey for the study of the Matsushiro Earthquake Swarm", No. 2 (1966).

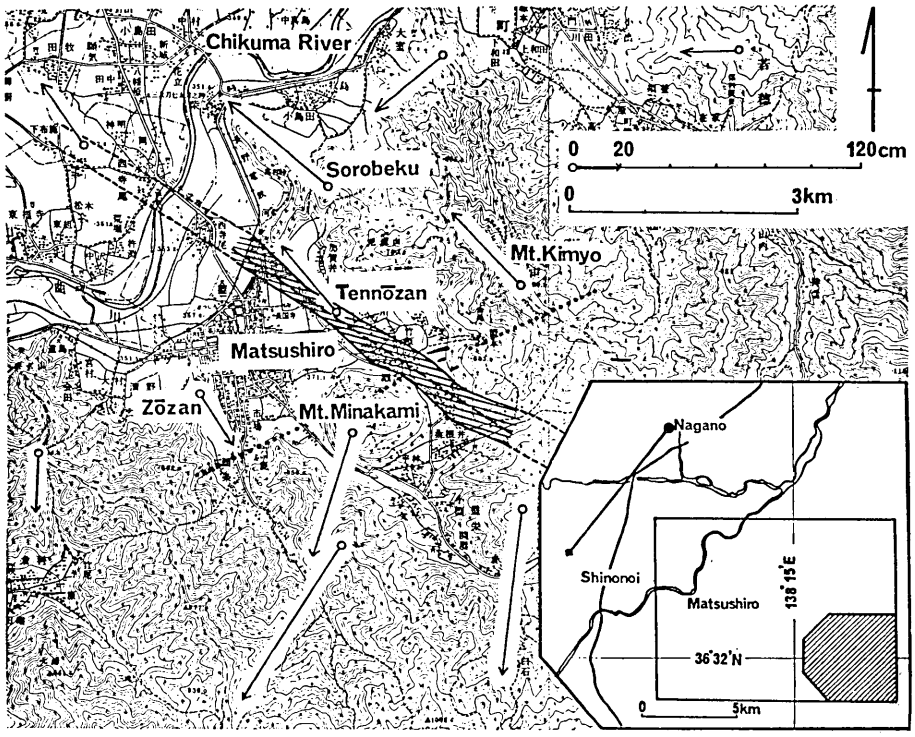

Fig. 50. Vectors representing horizontal displacement, 1904–1966, in the Matsushiro area.[11] A circle and an arrow in the smaller map indicate fixed triangulation point and direction. Hatched zone in the larger map shows location of the assumed buried fault according to surface evidence (cf. Fig. 12).

conjugate with the left-lateral one. Triangulation results (Fig. 50) also seem to support this interpretation. But, such a conjugate buried fault is not necessarily postulated for interpreting only the presence of right-lateral fissure zones, because they are distributed only in a fringe area of left-lateral fissure zones and do not define any elongate area like the fissured area defined by left-lateral fissure zones.

7. Location of the buried fault

General discussion

Individual cracks in the fissure zones are believed to be surficial features that merge with a continuous fault plane below a certain depth,

[11] Geographical Survey Institute, *loc. cit.*, 10).

say, less than about 10 metres. This is supported by the fact that vertical displacement took place parallel to the zone, rather than its component cracks (Fig. 15a).

Similarly, the faults represented by fissure zones are also believed to be shallow features which developed in the cover of unconsolidated deposits. Below a level deeper than some hundred metres, there would be a single continuous plane or narrow zone of faulting. This is suggested by the fact that 1) the fissure zones are distributed in a narrow extremely elongate fissured area in the manner similar to feather joints, 2) the areal horizontal and vertical displacement as indicated by surface evidences (Chap. 5) took place on, and on the extension of, the axis of the fissured area, and 3) on the northwest of the fissured area the axis of areal deformation lies on the extension of the axis of the fissured area, and not in the direction of individual fissure zones such as F_4 (Figs. 11 and 12).

The northwestern extension of the assumed fault would be traced by the zone of damage described in chapter 5. The belt of strong deformation defined by breakage of rice-field levees, damaged water pipe and breakage of roadside ditch lies just on the northwest extension of the assumed fault. The areal distribution of the deformation is uniaxial and symmetrical (Fig. 44) and proceeded simultaneously with the seismicity. Moreover, left-lateral sense of movement is apparent in the N10°W elongation, taking the direction of fault, N55°W, into consideration. Thus the fault would be located beneath the axis of the strong deformation belt.

Further northwestern extension would be defined by the stretch of deformed railroad track, judging from similarities in the sense of vertical and horizontal displacement with the assumed fault and from coincidence of rapid displacement with the high seismicity period. The two outer bending points in Fig. 45b would define the width of strong deformation belt.

From the foregoing evidence, the belt of strong deforamtion, which is 0.1～0.5 km wide (Fig. 12), can duly be regarded as the probable location of the buried earthquake fault. The length of the belt of strong deformation is at least 4 km, and possibly well over 7 km when the result of triangulation is taken into account. The axis is quite linear trending in a direction N55°W, as reproduced in Fig. 10. The left-lateral displacement along the assumed fault in the belt is quite consistent with the primary characteristics of the result of triangulation in the Matsushiro area, the result being reproduced in Fig. 50 along with the assumed fault.

The displacement shown in Fig. 50 is the accumulated sum between 1904–1966, most of which is believed to represent displacement associated with the present earthquakes. The horizontal displacement between three of twelve triangulation points repeatedly measured by Kasahara et al.[12] since October, 1965, amounts to almost the same value as the total amount during the period, 1904–1966 thereby indicating that it is largely associated with the present earthquakes. The result shown in Fig. 50 also suggests a possible right-lateral fault trending N65°±15°E and passing through the area of fissure zones F_6, F_{15} and F_{16} of right-lateral sense. The possible fault also reproduced in the figure by a dotted line.

Location of the fault in Tennōzan Hill

The zone F_4 runs about fifteen metres north of the triangulation point, Tennōzan, yet the point shows northwestward displacement suggesting that the axis of surface deformation should be located south of the point. This apparent contradiction will be interpreted as follows. Occurrence of ground cracks are strongly controlled by shallow local geology, as stressed already (p. 426), and zone F_4 is not an exception. The zone occurred on the ground surface of the yard of a shrine in its eastern part and a narrow inclined border between mulberry fields on the summit (Fig. 47). An adjacent hill slope is covered by brush, one of the worst conditions for occurrence and detection of ground cracks. This consideration, and the presence of ground cracks in a belt some three hundred metres wide in the fissured area suggest that F_4 may not be the only fissure zone in this hill and that other potential cracks may be expected on the nearby ground, including the south of the triangulation point. Moreover, extension of the axis of strong deformation in the adjoining rice-field south of the point (Fig. 47) is consistent with the horizontal displacement of the triangulation point. Thus, the triangulation point is judged to be situated within the belt of surface rupture and just north of the axis of the belt.

8. Estimation of displacement on the fault

General remarks

The measured amount of both horizontal and vertical displacement across the fissure zones is summarized in Table 3. It attains a maximum value in the middle of the zones, gradually decreasing to the end of the

12) K. KASAHARA and A. OKADA, *loc. cit.*, 7).

zone in those places where the end of the zone is observable. In this chapter, the displacement of the assumed buried fault is estimated from the surface evidences.

Horizontal displacement

Data on the total displacement in the belt of surface deformation are largely limited to a general north-south direction. General north-south extension of the ground is also suggested by opening of the component cracks of each fissure zones. The cracks strike in a narrow range between N60°E and N80°W, averaging N80°E in spite of diverse trends of individual fissure zones. This holds good for both left-lateral and right-lateral ones. If a uniform strain of the ground is assumed as a first approximation to the initial state of ground cracking, then N10°W, normal to the average strike direction, would represent the direction of maximum tension.

In the case of the railroad track (Fig. 45), the total length of rails increased as the result of replacement from September to December, 1966, by 404 mm in eastern rails and 310 mm in western ones. 357 mm, the average of the two, gives the approximate amount of extension of the ground in a direction N20°E in a horizontal span of about 500 m, although there are factors suggesting that this value could be somewhat larger or smaller. The clearances of joints seem to have become generally narrower as compared with the preseismic ones in the section concerned thereby tending to exaggerate the extension, whereas possible slip to some degree between rails and ground would tend to decrease it.

The roadside ditch provides another source of data on the horizontal displacement of the buried fault. In order to obtain a more realistic value of ground extension from the observed 324 mm extension of the ditch, two assumptions may be necessary. First, 20 mm is subtracted, because 2 mm opening per 10 m is a normal amount for this kind of concrete construction. Next, 100 mm is added to compensate for the missing segment of ditch represented by the broken line connecting open circles in Fig. 46. Thus, 404 mm or 40 cm is obtained as a plausible amount of extension in a N10°W direction at this place up to September 16, 1966.

Ground extension in a direction of about N10°W may also be estimated from the study of breakage of rice paddy levees. It amounts to 20 cm at most (Fig. 44). Because the levees are built originally separated into segments 10 to 30 metres long, this value of elongation (20 cm) would

represent a minimum value for the ground deformation.

Southeast of F_4, in the area of ground cracks, it is difficult to estimate an exact amount of displacement in the fissured area in any direction, because there is no such convenient construction as a railroad track or a concrete ditch extending across the entire fissured area. Even the displacement in a fissure zone is difficult to estimate, but if the amount in the entire fissured area is assumed to attain two times that on a single fissure zone, an assumption that seems to be reasonable from the distribution of fissure zones (Fig. 12), then 60 cm of strike-slip component and 34 cm of north-south extension are given from the amount at F_1-**a** (p. 439).

The amounts of ground extension in a direction of about N10°W as estimated in the foregoing section are consistently between 20～40 cm in spite of the varied ways of estimation. 30～40 cm would be a more plausible value if the various factors mentioned above are taken into account. If the displacement is assumed to be caused solely by strike-slip movement along the buried fault, then a strike-slip component of 42～56 cm is obtained, agreeing well with the value estimated from the triangulation data (Fig. 50).

On the other hand, this value of 30～40 cm extension in a N10°W direction amounts to only one-third of the extension, ca. 110 cm along the base line (about 3 km long) from Mt. Minakami to Sorobeku in the same direction, as revealed by electro-optical measurement[13]. The greater part of this difference may be ascribed to absorption of strain by the unconsolidated surface layers both inside and outside the belt of strong deformation. To a lesser extent it could possibly result from movement on a right-lateral fault or faults across the base line, although this is not sufficiently established by ground crack data. Part of the strain would have been stored as elastic strain. This is suggested by the contraction as revealed both by the electro-optical measurement (Fig. 49) and by ground crack measurement (p. 444).

Examination of the deformed railroad track possibly implies that there might be an opening component normal to the assumed fault, in addition to the component parallel to it. Although this rather unusual conclusion is not sufficiently established, it is, nevertheless, worth noting here. The deformed railroad track intersects the buried fault at an angle of 75° (Fig. 45). Ground extension in the direction of the track is estimated at about 36 cm as described earlier. If the extension is

13) K. KASAHARA and A. OKADA, *loc. cit.*, 7).

caused solely by the displacement in the direction of the fault, the displacement parallel to the fault should amount to over 130 cm. Actually, it is no more than 50 cm according to the naked eye observations of railroad personnel, and it can safely be regarded as considerably smaller than 130 cm. If the lateral offset of the track normal to its direction is taken as 30～50 cm, then the direction of displacement will be N20°～35°W. Since the trend of the fault is N55°W, the estimated direction N20°～35°W will indicate the presence of a normal component.

Vertical displacement

Because the down-thrown sides of left lateral fissure zones are all on the north of the zones in a narrow fissured area (Fig. 12), the northern side of the assumed fault is naturally assumed to have subsided relative to the south side.

The result of precise-levelling[14] shows that subsidence amounts to some fifteen centimetres. This is smaller than the maximum vertical displacement (30 cm) observed at fissure zones. In addition, the result shows that the area of surface faulting is situated in the central part of an upheaved area with a broad elongate dome-like shape nearly coinciding with the epicentral area and maximum vertical uplift of over 70 cm.[15] This might suggest that the vertical displacement along the fault is not so important as the horizontal one, in defining the nature of the earthquake fault.

9. Summary and Conclusion

1. During the two culminate periods of seismicity of the Matsushiro earthquake swarm in 1966, a system of ground cracks was formed in the centre of the epicentral area of the earthquake swarm. The system is not able to be interpreted as caused by simple upheaval of ground nor by landslide. The fissure zones consisting of a group of ground cracks show systematic horizontal and vertical displacement (Table 2) and are distributed in a narrow fissured area trending N55°W.

2. Ground cracks which are attributable to down slope movement of the ground, or landslides, also appeared in the same general area. Distinction of the cracks by responsible agents is made by careful field

14) I. TSUBOKAWA, A. OKADA, H. TAJIMA, I. MURATA, K. NAGASAWA, S. IZUTUYA and Y. ITO, "Levelling Resurvey associated with the Area of Matsushiro Earthquake Swarms. (I)," *Bull. Earthq. Res. Inst.*, **45** (1967) 265.

15) I. TSUBOKAWA et al., *loc. cit.*, 14).

observations on the basis of both *en cchelon* pattern of the component cracks in a fissure zone and relationship between the topographic relief and horizontal and vertical displacement along the cracks and zones (Table 3).

3. The ground cracks which are not attributable to landslide origin (Table 2) are best interpreted as resulting from left-lateral movement on a buried NW trending fault and a possible conjugate right-lateral fault. This interpretation is strongly supported by the result of triangulation conducted by the Geographical Survey Institute (Fig. 50). The assumed faulting is also consistent with the results of the first motion study of P waves and of the ground deformation as indicated by electro-optical measurements, covering an area of over 6 km^2 including the fissured area.

4. Continuous measurement for more than 150 days of both paths and amounts of displacement on ground cracks and fissure zones by various types of apparatus also supported the fault interpretation, and revealed their mode of displacement in function of time. The time rate of displacement is quite similar at six different stations (Fig. 42), agreeing well with the rise and fall of seismicity and of the horizontal (and vertical) land deformation as revealed by electro-optical measurements (and precise levelling) (Fig. 49).

5. The assumed left-lateral fault trends around N55°W and the length is over 4 km, possibly 7 km, taking the result of triangulation into account. According to the study of ground cracks, deformation of a railroad track (Fig. 45), roadside-ditch (Fig. 46), water pipe (Fig. 47) and concrete levees in rice-fields (Fig. 44), the surface displacement caused by the buried fault is an extension of some 40 cm in a N10°W direction. There is an indication that there may be an opening component normal to the fault besides the component parallel to it.

6. While the strike-slip component of the faulting is estimated to amount to 40～60 cm, vertical displacement attains about 15 cm in a belt of a few hundred metres in width. A maximum amount of displacement on a fissure zone which was measured at the middle of the zone, is 30 cm at largest in both vertical and lateral components.

Problems to be studied are 1) three dimensional relationship between surface ruptures (*en echelon* cracks in fissure zones and *en echelon* fissure zones in the fissured area) and buried fault, 2) the relationship between the displacement of the fault and the location and magnitude of the individual earthquakes, and 3) the situation of the left-lateral fault, pointed

out by the present study, in the geologic structure and history of the epicentral area. In connection with the last problem, the geology of the fissured area was described in the companion paper by MATSUDA.[16]

Acknowledgement: The writers are grateful to residents of Matsushiro for information regarding ground cracks, especially to Mrs. Makie SAITO, Mr. Koichi AIZAWA, Mr. Shuichi OGAWARA, Mr. Kengo NAKAMURA and Miss. Yasuyo NISHIMURA for their help with daily measurements, to Mr. Zenji KUMAI, Mr. Tomokazu NAKAMURA and Mr. Yoshiteru AOKI for kindly offering their ground for measurement stations, to Mr. Isao KASUGA for the photograph (Fig. 48) and for data regarding his water pipe (Table 5), to the personnel responsible for the railroad maintenance of the Nagano Electric Railway Co. Ltd., Messrs. Kaname KANABAKO, Takeo SHIOZAKI and Yoichi IIJIMA for offering the railroad data, to the town office for providing support for survey, and to Prof. R. MORIMOTO for giving many facilities to the writers. They are also indebted to Drs. Kazuo HOSHINO, Tokihiko MATSUDA and George PLAFKER for kindly reading the original manuscript, to Dr. T. MATSUDA and Mr. H. TAKAHASHI for their help in temporarily joining the field survey. Part of the present study was supported by a grant given by the Ministry of Education.

16) T. MATSUDA, "Geological Aspect of the Matsushiro Earthquake Fault", *Bull. Earthq. Res. Inst.*, **44** (1967), 624, (in Japanese with English resumé).

24. 横ずれ断層によると考えられる松代の地割れ群 II—松代地震断層

地震研究所 中村一明・恒石幸正

1965 年 8 月に始まつた松代地震群は翌 1966 年の 4 月および 8 月—9 月に最盛期を迎え，震央域では水平・鉛直方向の地殻変動，地割れの出現，地辷りの発生，異常な地下水の湧出などの地変が続いた．筆者らはこれらの現象のうち主として潜在地震断層の発生を指示すると考えられる地割れについての研究を行なつた．

第 1 報において 1966 年 6 月までの結果を報告し，地辷りによるとは考えられない地割れの分布およびその変位方向などから基盤岩中に潜在する北西—南東方向の横ずれ地震断層を皆神山北東方に推定した．その後の事態の進展に伴う諸観測・観察の結果は，ますます潜在断層の存在を確実なものとした．本稿ではこれまでに生じた地割れの分布と記載，それらの地割れの成因による区分，変位量および方向の連続観測の方法および結果の記載，その他の水平変動を指示すると考えられる地変の記載，以上の結果に基づく地震断層の仮説の検討，こうして推定された潜在断層の位置の推定と変位量の算定を行なう．

1967 年 3 月までに筆者らが確認した，割れ目帯 fissure zone（小さな雁行する割れ目 ground crack の集合のこと．なお地割れという言葉は，ここでいう割れ目，割れ目帯の区別なく一般的な語として使用する）の分布は Fig. 11 に示されている．これらの割れ目帯は，個々の割れ目の配列様式，分布の場所および地形の起伏との関係によつて横ずれ断層起源と予想されるもの（A 型）と，小地域内での表層現象である地辷り，すなわち重力の作用に起因すると判断されるもの（B 型）とに分類される．A 型割れ目帯の特徴は，それを構成する個々の小さな割れ目が全体を通じて一様な雁行配列をすること，皆神山北東地域で北西方向にのびる狭い地帯（本稿ではこれを地割れ地帯 fissured area とよぶ）の中にだけ分布すること，ほぼ直線的に伸び起伏と全く関係をもたないこと，左横ずれ雁行を示すものは北東側が，右横ずれのものは南東側が最大 30 cm 沈下しているなどである．これに対して B 型割れ目帯はつねに，地形的に低い側の土地が低い方へ，時に回転を伴いながらずり下ることによつて生じたとみなされる特徴をそなえている．以上のことは Table 2 にまとめられている．こうして分離された 16 本の A 型割れ目帯の規模，変位量・方向等は Table 3 にまとめられている．F_1～F_4 の四つの割れ目帯はすでに 4 月の活動期に発生したもの (Fig. 2) であるが，8 月末頃よりこれらはさらに変位量を増大し，全長ものびた．同時にさらに 7 本の左横ずれを示す割れ目帯と 3 本の右横ずれを示すものが加わつた．左横ずれを示すものは F_1～F_4 の分布によつてすでに定められていた幅狭い地帯の内およびその延長上に雁行して分布し，右横ずれを示すものはこの地帯中央部の北東縁にあり，両者は共役的関係にあるようである (Figs. 10, 11, および 12).

これらのうち 5 本の割れ目帯上の 6 ヵ所に観測点が設けられ 1 日 1～2 回の間隔で割れ目もしくは割れ目帯の変位が測定された．より多くの場所ですみやかに観測を始めるため最初は非常に簡単な方法で変位量および変位の方向経路の測定を行ない，後に順次改良していつた．測定結果 (Figs. 32-42) を要約すれば次のようになる．

1. 変位量の時間的変化は，6 測点 (**a**～**f**, Fig. 11) を通じて非常によく似ている．
2. 地震活動の消長にほぼ対応して地割れも 4 月と 8 月—9 月の二つの時期に大きな変位を示した．8 月—9 月の活動期には 4 月に比して約 1.5 倍の変位量を示した．
3. 二つの活動期にはさまれた期間の変動は全体的には小さいが測点 F_4-**e** では他の測点よりも大きな変位がみられた．この測点は中新統の岩盤まで約 1 m しかない場所に設けられているが，他の測点は数 10 m以上の厚さをもつ扇状地堆積物の上にある．
4. 8 月—9 月の活動期の後は，量は少ないが構成割れ目の閉じる向きに変化している（ほぼ南北方向の収縮）．
5. 測点 F_4-**e** では地割れ地帯延長上に震源をもつ二つの大きな地震時 (8 月 20 日 M=4.4 と 9 月 6 日 M=5.0) に急激な変位が認められた．この変位は，9 月 6 日の例について，一瞬のうちに起こるのではなく，数時間かけて進行する過程が追跡された (Fig. 40).

6. 割れ目帯を構成する割れ目は最初は単純な開口によつて形成され，のちにしだいに横ずれ成分を増している．割れ目帯の変位についても同様のことがみられる．最も明瞭な例は，地割れ発生後の早い時期に変位計をとりつけた測点 F_6-f である (Fig. 41).

地割れの観測結果と光波測量の皆神山—可候基線の距離変化とを比較すると (Fig. 49) 量は 1/5 程度であるが時間変化の仕方は地割れの値が，一定方向内の変化でないにもかかわらず非常によく似ている．9 月以降にみられる南北方向の収縮も，それが光波測量の結果にもあらわれているところから一旦開口した割れ目が単に表層的に閉じただけのものではないこともわかる．

割れ目帯 F_4 の生じた岡の北西方は水田に利用されている低湿地のため，地割れは発見できなかつたが，コンクリートの畔や道路の側溝に系統的な割れ目が生じている．南北方向の畔や側溝は割れて開口しているが，東西方向のものはたとえ割れていても開口を示さない (Fig. 43). Fig. 44 は南北方向の畔 10 m 当りの開口量を mm 単位で表わし，等開口率線を描いたものである．変形は北西方向の直線的な領域に集中し，側方へは対称的に減少している．畔の開口方向との関係から左横ずれの成分が認められる．

さらに北西の松代駅北東方で長野電鉄河東線松代駅～金井山駅間のレールに，地震に伴つた変位がみとめられる．Fig. 45a に示される場所で軌条は異常に引延ばされ，かつわずかながら S 字形に変形している (Fig. 45b, c)．この現象は 1966 年の 4 月頃から認められはじめたようであり，その後 8-9 月に至つてますます進行したため 9 月，11 月に 1 本ずつより長いレールとの交換，12 月には区間全体にわたつて軌条の遊間整理作業が行なわれた．

以上の事実より，まず地割れについては，A型割れ目帯は前記の観測結果の共通性の外に，水平・鉛直両成分が調和的に変化すること，構成する個々の割れ目の方向が，割れ目帯の方向や横ずれ方向にかかわりなく平均 N80°E の方向に比較的よくそろつていること (Table 3)，横ずれ方向の同じ割れ目帯はよく方向がそろつていることなどの性質によつて特長づけられ，共通の成因をもつていることが裏づけられる．さらに地割れ地域の北西延長にみとめられる地変をも同時に説明するにはこの地帯の地下に左横ずれ断層を想定するのが一番もつともらしい．こうして推定された潜在断層を松代地震断層とよぶ．F_1, F_2 等の個々の割れ目帯も断層とよんでもよいかもしれない．しかし本稿では，潜在断層が本源的なものであり，割れ目帯は沖積層中の表層的なものであると考えられるので，断層とはよばない．

地震断層は幅 0.1～0.5 km，長さ 4 km 以上の第 12 および 50 図に示された強く変形した地帯を通つていると考えられる．走向は N55°W である．このような断層が形成される応力条件では東西方向に最大，南北方向に最小の圧縮主応力軸があり，これは松代地震群の発震機構とよく合致する．国土地理院によつて行なわれた三角測量の結果 (Fig. 50) は，この研究によつて推定された断層の存在を強く支持している．

断層の変位量を算定するために利用できる資料は南北方向のものが多い．以下これらの資料を北西部から列挙する．

1. 長野電鉄の軌条の伸びの量は 500 m の区間で約 36 cm (N20°E) である (Fig. 45a).
2. 道路の側溝から得られた伸長量は 100 m の区間で約 40 cm (N10°W) である (Fig. 46).
3. 上の側溝の 100 m 東では，一陽館に通ずる水道管が南北方向に埋設されている．この水道管は少なくとも 9 カ所で土地の伸長のため切断された．開口量の和は約 23 cm (N10°W) である．
4. コンクリート畔の割れ目の開口量から求めた南北伸長は約 20 cm (N10°W) である
5. 地割れ地域での正確な評価は困難である．分布図 (Fig. 12) から判断して割れ目帯中央部の変位の 2 倍が地割れ地域の変位を与えるものとして，F_1-a のコンクリートたたきの値を使えば，約 60 cm (N55°W) 約 34 cm (N-S) となる．

以上の量のうち 3. は水道管の未発見の切れ目がまだ存在する可能性があること，4. の畔は南北向方にひとつづきのものではなく長さ 10～30m 程度の畔にはじめから分れているため不連続部分の開口量を落していることにより，おそらく過小評価された値が得られているのであろう．

これらの事情を考慮に入れると断層変位による土地の N10°W 方向の伸長量として 30～40 cm の値が妥当となろう．この値を用いて N55°W 方向の断層の走向に沿つた変位量を求めると 42～57 cm となる．三角測量の結果 (Fig. 50) から読みとられる断層に沿つた変位の成分もほぼこの程度である．

一方光波測量の皆神山—可候基線（約 3 km）の変化および三角測量によるこの区間の N10°W 方向の伸長は約 1 m に達する．30～40 cm と 1 m との伸長量のちがいは，測線長の相異を考慮すれば被覆層中の割れ目を生じない塑性的な変形によつて説明されよう．一部は強く変形した地割れ地帯の外側の地域でも肉眼ではみえないような変形が散在していることを示すのであろうし，一部は地下に弾性歪として蓄えられたものかも知れない．9 月以降の収縮もこのことを示す可能性がある．また三角測量の結果から象山—皆神山間に，右横ずれの割れ目帯付近を通つて北東方向の右横ずれ断層（Fig. 50 の点線）が潜在している可能性が考えられる．しかしこの断層についてはその他の証拠がないため確かに存在するとはいいきれない．

断層の鉛直成分については割れ目帯の観察および水準測量の結果から断層は全体としてはドーム状に隆起する地域内にあつて北東側が相対的に 10～20 cm 落ちていることが推定される．

謝辞: この研究に当つて松代町在住の多くの方々に大変お世話になつた．特に斎藤まき江氏，西村泰代氏，相沢耕市氏，小河原修一氏，中村健吾氏には一年近くもの間，毎日測定をしていただいた．熊井善治氏，中村智万氏，青木元光氏は観測のための土地を貸してくださつた．また春日功氏は水道管の切断に関する資料（Table 5）と写真（Fig. 48）を提供して下さつた．青山悦男氏はじめ牧内の地元り現地対策本部の方々は地割れ分布地域の案内をして下さつた．長野電鉄保線課・保線区・松代保線分区の方々，特に金箱要課長・塩崎武男区長・飯島与一分区長には保線上の資料を種々御教示いただいた．松代町役場の方にもいろいろ調査に便宜をはかつていただいた．地震研究所の森本良平・松田時彦・高橋春男の諸氏は数回にわたり野外調査に参加協力され，討論して下さつた．地質調査所の星野一男・合衆国地質調査所の George Plafker・地震研究所の松田時彦の各氏には原稿を読んで批判していただいた．費用の一部には文部省科学研究費をあてた．以上の方々および諸機関に厚く御礼申しあげたい．